AFRL-AFOSR-UK-TR-2020-0011

Design & Modeling of a Dispersive Pulse Compressor based Frequency Tunable HPM System

Kevin Ronald
UNIVERSITY OF STRATHCLYDE VIZ ROYAL COLLEGE OF SCIENCE & TECHNOLOGY
16 RICHMOND STREET
GLASGOW, G1 1XT
GB

05/14/2020
Final Report

DISTRIBUTION A: Distribution approved for public release.

Air Force Research Laboratory
Air Force Office of Scientific Research
European Office of Aerospace Research and Development
Unit 4515 Box 14, APO AE 09421

REPORT DOCUMENTATION PAGE

Form Approved
OMB No. 0704-0188

The public reporting burden for this collection of information is estimated to average 1 hour per response, including the time for reviewing instructions, searching existing data sources, gathering and maintaining the data needed, and completing and reviewing the collection of information. Send comments regarding this burden estimate or any other aspect of this collection of information, including suggestions for reducing the burden, to Department of Defense, Executive Services, Directorate (0704-0188). Respondents should be aware that notwithstanding any other provision of law, no person shall be subject to any penalty for failing to comply with a collection of information if it does not display a currently valid OMB control number.
PLEASE DO NOT RETURN YOUR FORM TO THE ABOVE ORGANIZATION.

1. REPORT DATE *(DD-MM-YYYY)*	2. REPORT TYPE	3. DATES COVERED *(From - To)*
14-05-2020	Final	30 Sep 2018 to 29 Sep 2019

4. TITLE AND SUBTITLE
Design & Modeling of a Dispersive Pulse Compressor based Frequency Tunable HPM System

5a. CONTRACT NUMBER

5b. GRANT NUMBER
FA9550-18-1-7014

5c. PROGRAM ELEMENT NUMBER
61102F

6. AUTHOR(S)
Kevin Ronald, Alan Phelps

5d. PROJECT NUMBER

5e. TASK NUMBER

5f. WORK UNIT NUMBER

7. PERFORMING ORGANIZATION NAME(S) AND ADDRESS(ES)
UNIVERSITY OF STRATHCLYDE VIZ ROYAL COLLEGE OF SCIENCE & TECHNOLOGY
16 RICHMOND STREET
GLASGOW, G1 1XT GB

8. PERFORMING ORGANIZATION REPORT NUMBER

9. SPONSORING/MONITORING AGENCY NAME(S) AND ADDRESS(ES)
EOARD
Unit 4515
APO AE 09421-4515

10. SPONSOR/MONITOR'S ACRONYM(S)
AFRL/AFOSR IOE

11. SPONSOR/MONITOR'S REPORT NUMBER(S)
AFRL-AFOSR-UK-TR-2020-0011

12. DISTRIBUTION/AVAILABILITY STATEMENT
A DISTRIBUTION UNLIMITED: PB Public Release

13. SUPPLEMENTARY NOTES

14. ABSTRACT
The potential for increasing the range of frequencies which can be compressed by a dispersive, hollow, helically corrugated, waveguide has been investigated. A three-fold helical corrugation was investigated since initial analysis revealed that five-fold corrugation schemes, although certainly supporting higher power levels, would be difficult to extend in frequency range. Analytical methods, time domain and eigenmode computer simulations were used to predict the dispersion of the helically corrugated waveguide for the two distinct circular polarisations (which exist due to the chirality of the waveguide). These were found to be in excellent agreement with the experimental measurements. Critically the measurements showed that the uncoupled polarisation had almost no modification to its dispersion when compared to the behaviour of a smooth waveguide.

15. SUBJECT TERMS
dispersive pulse compressor, high power amplifier, RF pulse compression, gyro-Traveling Wave Tube, high power microwave

16. SECURITY CLASSIFICATION OF:			17. LIMITATION OF ABSTRACT	18. NUMBER OF PAGES	19a. NAME OF RESPONSIBLE PERSON
a. REPORT	b. ABSTRACT	c. THIS PAGE			LOCKWOOD, NATHANIEL
Unclassified	Unclassified	Unclassified	SAR		19b. TELEPHONE NUMBER *(Include area code)* 011-44-1895-616005

Standard Form 298 (Rev. 8/98)
Prescribed by ANSI Std. Z39.18

Design & Modeling of a Dispersive Pulse Compressor based Frequency Tunable HPM System

Final report, Contract number FA9550-18-1-7014

28th December 2019

Lead Author: Dr. Alan R. Young,

Principal Investigator: Dr. Kevin Ronald,

Co-Investigator: Prof. Alan D.R. Phelps

All Department of Physics, University of Strathclyde, Glasgow, G4 0NG

Period of Performance: 30.Sept.2018-29.Sept.2019

Distribution A Distribution Approved for Public Release: Distribution Unlimited

Executive Summary

The potential for increasing the range of frequencies which can be compressed by a dispersive, hollow, helically corrugated, waveguide has been investigated. A three-fold helical corrugation was investigated since initial analysis revealed that five-fold corrugation schemes, although certainly supporting higher power levels, would be difficult to extend in frequency range. Analytical methods, time domain and eigenmode computer simulations were used to predict the dispersion of the helically corrugated waveguide for the two distinct circular polarisations (which exist due to the chirality of the waveguide). These were found to be in excellent agreement with the experimental measurements. Critically the measurements showed that the 'uncoupled' polarisation had almost no modification to its dispersion when compared to the behaviour of a smooth waveguide. This was true at frequencies close to that where the 'coupled' polarisation showed strong variation in the dispersion and for a very substantial frequency range both above and below that band. This allows a second pulse compressor to be combined in series and using the opposite polarisation, tuned to an alternative frequency range. It is not possible to implement this for two series combinations of pulse compressor in the same polarisation since for the 'coupled' polarisation a strong stopband exists just above the region of strong dispersion. This increases the usable range from around 500-600MHz around 9.3GHz by a factor of around two (it is not essential that the two bands be exactly contiguous).

Simulations, verified by experimental measurements have shown that a novel polariser can provide the required circularly polarised input signal over a bandwidth sufficient to enable the series combination of the two compressors. Simulations have been undertaken to assess the field enhancement over smooth waveguide induced by the helical corrugation on the waveguide walls. From these, and drawing on material in the literature the peak power capability of the corrugated waveguide was assessed. Allowing for the short pulse duration, the peak power handling was estimated to be ~ 5MW in dry air, but potentially much higher in vacuum, up to GW level.

Publications on CNT film have been reviewed- it seems likely the best short term advantage to dispersive pulse compression from this technology would be to use the CNT as a light weight mechanical support, internally coated with metal. A next step would be to make a smooth wall metal-on-CNT waveguide for experimental test against conventional waveguide.

Distribution A Distribution Approved for Public Release: Distribution Unlimited

Table of Contents

Distribution A Distribution Approved for Public Release: Distribution Unlimited

Table of Figures

Distribution A Distribution Approved for Public Release: Distribution Unlimited

Distribution A Distribution Approved for Public Release: Distribution Unlimited

1. Introduction

Pulse compression of microwave pulses using a dispersive waveguide is an effective technique for producing short high peak power pulses from frequency-chirped longer duration lower power pulses. The technique was investigated in the radio and microwave spectrum for application in pulse wideband RaDAR where the technique was typically applied in the receive side of the system. This allows weak return signals to be observed above the background. The technique is also used in laser physics where the laser gain medium and optics cannot tolerate the peak signal strength- a short pulse signal can be dispersively stretched into a long chirped pulse which may be more readily manipulated and amplified then recompressed. The effect is dependent (in each case) on there being significant change in effective group velocity with frequency. This means that although smooth waveguides may be used for pulse compression in the microwave spectrum, and certainly have high peak and average power handling capability their dispersion is not ideal for this application. There are two problems associated with using a smooth bore waveguide as a pulse compression medium. Firstly the group velocity is only a strong function of frequency close to cut-off, and therefore to optimise performance the input signal will need to be as close to cut-off as possible. However any component of the signal below the cut-off will be reflected back to the driver, potentially interfering with its operation, whilst the behaviour of the overall system will be highly sensitive to relatively small perturbations in the waveguide's transverse dimensions. Secondly, close to cut-off the group velocity is low meaning that losses experienced will be greater than desired.

Both these problems can be addressed using a helical corrugation in the inner wall of a nominally cylindrical waveguide[i,ii,iii] as the pulse compressor[iv,v,vi]. A helical waveguide has an inner surface defined in cylindrical coordinates by the formula

$$r(\varphi, z) = r_0 + l\cos(m_B\varphi + k_B z)$$

Where r_0 is the mean radius of the waveguide, l is the corrugation amplitude, m_B is the azimuthal number of the Bragg periodicity vector, or the fold of the helix and k_B is the axial component of the Bragg periodicity vector and is given by:

$$k_B = \frac{2\pi}{d}$$

Distribution A Distribution Approved for Public Release: Distribution Unlimited

Where d is the axial period. figure 1 shows a model of a single period of helically corrugated waveguide.

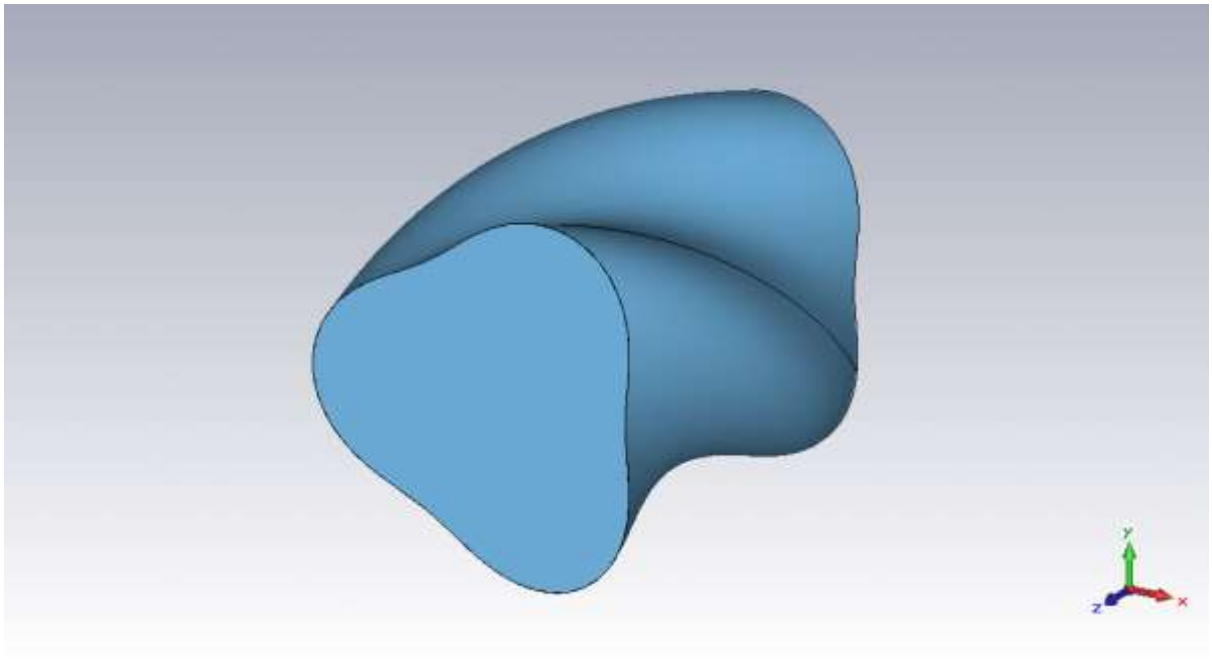

Figure 1 Single period of helical waveguide

The corrugation of the waveguide couples together circularly polarised modes which satisfy coupling 'Bragg' relationships between their wavevectors and the structure of the waveguide. The axial wavevectors of the coupled modes must be related by k_B and the azimuthal mode indices are related by m_B, the azimuthal order of the corrugation. The effect of this is that an infinite number of degenerate modes are formed (the space harmonics) spread in the wavevector axis by k_B and coupling arises between these modes and higher order modes which satisfy the relationship:

$$m_2 = m_1 - m_B.$$

Here m_2 and m_1 are the azimuthal indices of the two modes being considered. Negative azimuthal indices indicate that the direction of rotation of the mode polarisation is reversed. Hence a three fold corrugation will couple a counter rotating $TE_{1,1}$ dipole like mode with a $TE_{2,1}$ quadrupole like mode. In the present project the potential for enhancing the frequency flexibility of the pulse compressor was considered. By choosing carefully the wavegujde corrugation dimensions, the coupling of these modes can be tuned to provide a knee in the dispersion relation, well away from cut-

Distribution A Distribution Approved for Public Release: Distribution Unlimited

off, over which the group velocity changes rapidly with frequency and to control the variation of the group velocity with frequency, allowing the dispersion to be optimised. A pulse compressor based on such a dispersive structure has a constrained spectral range, of order 5% of the overall carrier frequency over which the group velocity has the desirable variation with frequency, and the intention in the present work was to explore ways in which this could best be extended whilst retaining the high performance 'designed' region for pulse compression operation.

2. Methods, Assumptions and Procedures

The primary method used was numerical simulation, benchmarked by experimental test of the behaviour of critical components. CST Microwave Studio was the main simulation code used in this project. It uses a Finite Integration Technique to calculate the time dependent electric and magnetic fields in microwave structures. A model of the helical waveguide was built in CST Microwave Studio and is shown in figure 2.

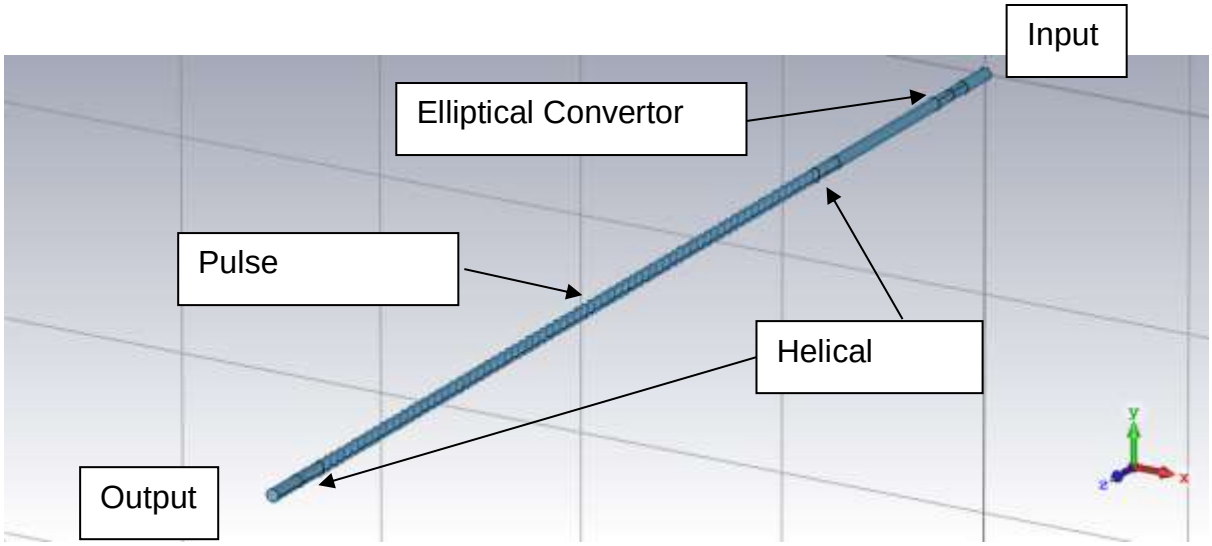

Figure 2 CST Microwave Studio Model of 3-fold pulse compressor.

The experimental method used was measurement by Vector Network Analyser [VNA] of important components of the system. A VNA measures the relative amplitude and phase of a signal transmitted through and reflected from a device under test. To undertake this measurement the analyser must be calibrated to remove the electrical length, reflections and responses of all components up to reference planes on each of the analysers' two ports. For this measurement these were defined to be the last

Distribution A Distribution Approved for Public Release: Distribution Unlimited

section of WG16 waveguide bracketing the components under test. This allowed the calibration to take advantage of precision shorts, zero length ‘throughs’ and most importantly -40dB precision matches. This allowed the analyser to be calibrated in a ‘Thru’-Reflect-Match’ approach for 10 term error correction up to the final WG16 ports. This is illustrated in figure 3.

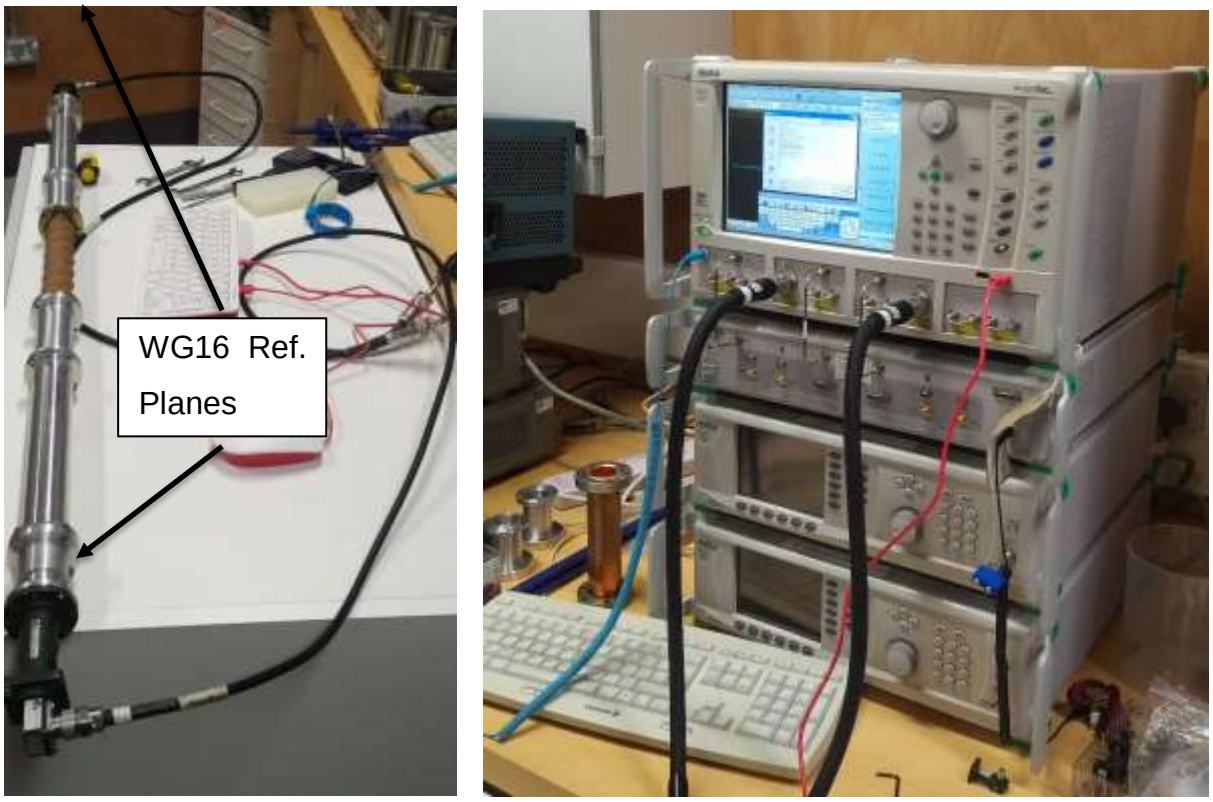

Figure 3 Experimental setup to measure dispersion of a section of helical waveguide, a similar configuration was used for all other components measured in this report.

The LHS of figure 3 shows the components being measured between the reference planes where the analyser was calibrated, whilst the RHS shows the network analyser being used for the measurements.

Typically various convertors were required to adapt from the WG16 ports to the correct ports for the devices which were to be measured. In each case these devices were designed and/or selected to have minimal reflection and therefore primarily impacted on the overall electrical length of the important ‘through’ measurements. This was compensated by measuring the system with ONLY the convertors installed and subtracting the phase shift of this reference measurement from the phase shift

Distribution A Distribution Approved for Public Release: Distribution Unlimited

recorded when the convertors were integrated with the components to be measured, thus extracting the phase shift induced by the component of interest.

Alternatively when measuring the performance of circular polarising components, providing the reflections are low, only the phase difference perceived by the two linear polarisations are relevant and therefore the two measurements can serve as their own 'references' by taking the difference as the relative polarisation of the wave is changed.

Discussion with AFOSR experts indicated the X-band region was particularly interesting for this project. The ABP laboratory has considerable prior experience working in this frequency range. The pulse compressor investigated as a benchmark for this project had a mean radius of 14.68mm, a 3 fold corrugation of depth 1.4mm, an axial period of 28.9mm with a length which could be adjusted to refine the compressor performance.

3. Results and Discussion

The primary focus of the research undertaken is to explore the potential to extend the known high performance of helically corrugated waveguide pulse compressors to extend the frequency range over which a given device can be reasonably optimised. The focus of the research was therefore on a three-fold helically corrugated pulse compressor, with dimensions noted in section 2. At either end of the pulse compressor are helical tapers, each three periods long, that taper from smooth waveguide of radius 28.9mm to the helically corrugated section. The helical tapers are to reduce reflections that would occur from the impedance (and spatial field structure) mismatch that would arise from a step change from smoothbore waveguide to helical waveguide.

Analysis also considered the potential for a five-fold helically corrugated waveguide[vii,viii]- these couple together two relatively high order modes and can be optimised to mitigate the surface electric field strength for a given carried EM power level. These devices are extremely attractive, however two serious problems conspire to make it difficult to extend the spectral coverage. Firstly the mode convertors required to excite the input higher order mode from a lower order mode typically output by an appropriately powerful source (e.g. $TM_{0,1}$ from a relativistic Backward Wave Oscillator or $TE_{1,1}$ from a fast wave amplifier) are also rather tightly bandwidth limited.

Distribution A Distribution Approved for Public Release: Distribution Unlimited

The second issue is that there is a relatively dense mode spectrum available in such an overmoded structure, so that operating it outside of a narrow spectral range is likely to excite some of these other modes - to the severe detriment of the behaviour of the overall system.

Three-fold compressors on the other hand require relatively simple and wideband transitions from the modes excited by the two types of wideband “chirp capable” high power sources described above. Specifically no mode convertor is strictly needed from the output of a powerful type of gyrotron amplifier based on similar 3-fold helically corrugated waveguide[i,ii,ix], whilst the convertor for a backward wave oscillator would be a simple serpentine. Moreover when operating out of band, the relatively sparse mode spectrum of the smaller three-fold compressor structures means that one has greater control over the modes that may be excited. The overall structure for such a compressor is illustrated in figure 2.

An ‘elliptical’ convertor- essentially a microwave quarter wave plate - converts the linearly polarised input to circularly polarised as the helix only strongly couples circularly polarised input ‘dipole’ $TE_{1,1}$ modes rotating counter to its internal geometry to the quadrupole $TE_{2,1}$ mode. The co-rotating $TE_{1,1}$ mode would be coupled to the much higher order $TE_{4,n}$ and $TM_{4,n}$ modes. These are very strongly cut-off at the frequencies of interest and therefore the co-rotating dipole like mode is scarcely perturbed by the helically corrugated waveguide in terms of its dispersion (and indeed is relatively weakly perturbed in terms of its field structure).

The input for the model is in the top right hand corner in figure 2 (although it should be noted that all components here are reciprocal - so the direction could equally be reversed). There is a region of smooth waveguide from the input to the elliptical convertor. There is another section of smooth bore waveguide from the elliptical convertor to a helical taper. The model is finished with a small section of smooth bore waveguide.

3.1 Input Pulse Production

Waveguide pulse compressors work by exploiting some transmission medium where the group velocity of a wave is frequency dependent. This means that for a given pulse compressor dispersion there is an optimum input pulse of particular length and

Distribution A Distribution Approved for Public Release: Distribution Unlimited

sweep in frequency. In order to calculate the optimum input pulse it is necessary to first calculate (or measure) the dispersion of the pulse compressor. For this project three methods were used to calculate the dispersion of the pulse compressor, one analytical and two numerical as well as a direct measurement using a VNA.

3.1.1 Analytical Dispersion Calculation

The helical structure of the proposed pulse compressor works by creating an operating mode that is composed of a coupling of two modes. For the 3-fold helix the two modes are the $TE_{1,1}$ and $TE_{2,1}$ mode. The dispersion is given by:

$$(k^2 - k_z^2 - k_{\perp 1}^2)(k^2 - (k_z - k_B)^2 - k_{\perp 2}^2) = 4\kappa^2 k_0^4$$

Where k is angular frequency divided by the speed of light, k_z is the axial wavenumber, $k_{\perp 1}$ is the cut-off wavenumber of the $TE_{2,1}$ mode, $k_{\perp 2}$ is the cut-off wavenumber of the $TE_{1,1}$ mode, κ is the coupling coefficient, which is dependent on the amplitude of the corrugation and k_0 is the wave vector of exact Bragg resonance. It is possible to solve this equation using a numerical root finder and hence determine the relationship between angular frequency and axial wavenumber for the coupled mode.

Distribution A Distribution Approved for Public Release: Distribution Unlimited

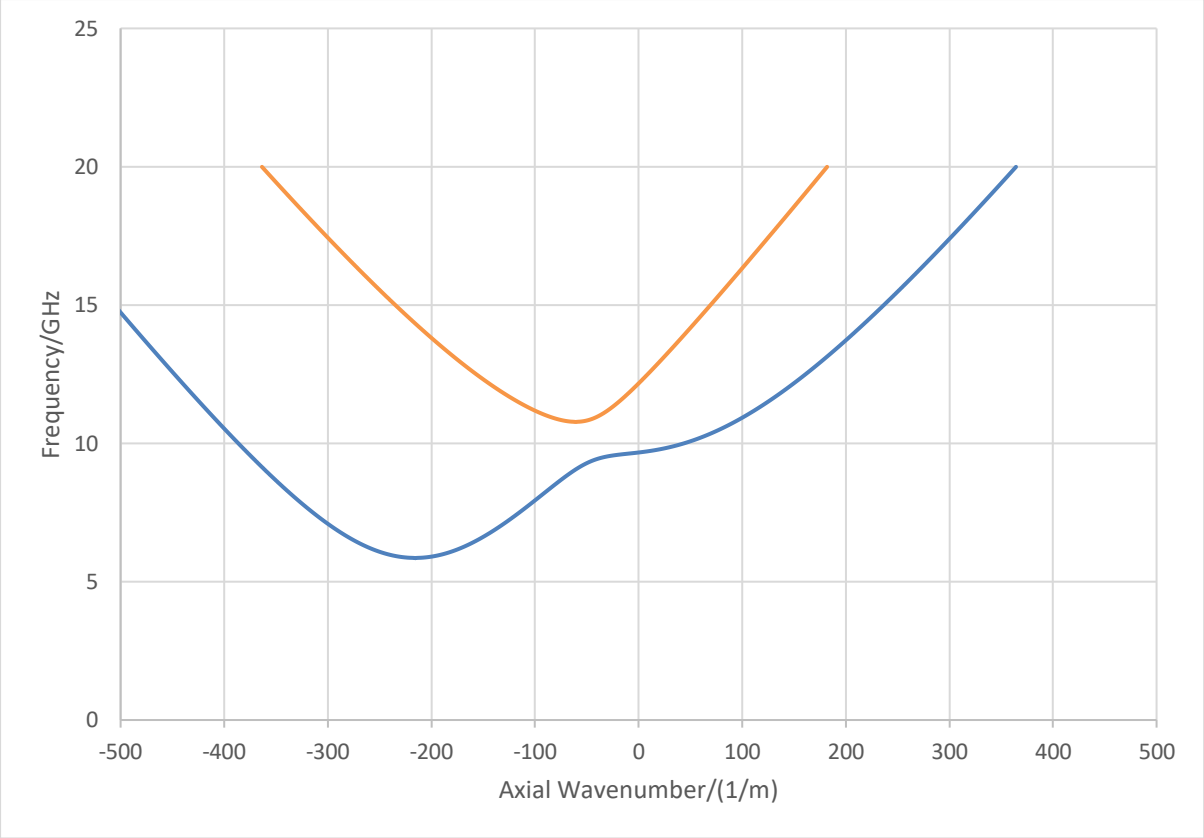

Figure 4 Dispersion of 3-fold helical waveguide

3.1.2 Numerical Calculation of Dispersion

The method described in the previous section is based on perturbation theory. This makes the assumption that the electromagnetic fields in the complex structure can be represented by coupling together solutions for an equivalent smooth waveguide offset by the axial wavevector of the corrugation, and allowing for the corrugation through the coupling parameter. The method has validity constraints, especially where the corrugation amplitude becomes large (assessed as a fraction of the mean diameter). It is possible to obtain a solution to the dispersion of the waveguide numerically.

It should be noted however that although the dispersion of the helically corrugated waveguide is critical to the pulse compression process, the essential components required to launch and receive the signal also have a dispersive behaviour (usually quite weak, the importance of which will vary with the frequency compared to the cut-off frequency of the waveguide). The optimum injection pulse chirp can therefore be determined by establishing the dispersion of the entire apparatus. A computation was

Distribution A Distribution Approved for Public Release: Distribution Unlimited

undertaken using the numerical simulation code CST Microwave Studio to predict this total dispersion of the assembly.

Using a transient model a Gaussian pulse over the frequency range of interest is injected into one end of the pulse compressor and the phase shift of the S-parameter at the output is measured (figure 5).

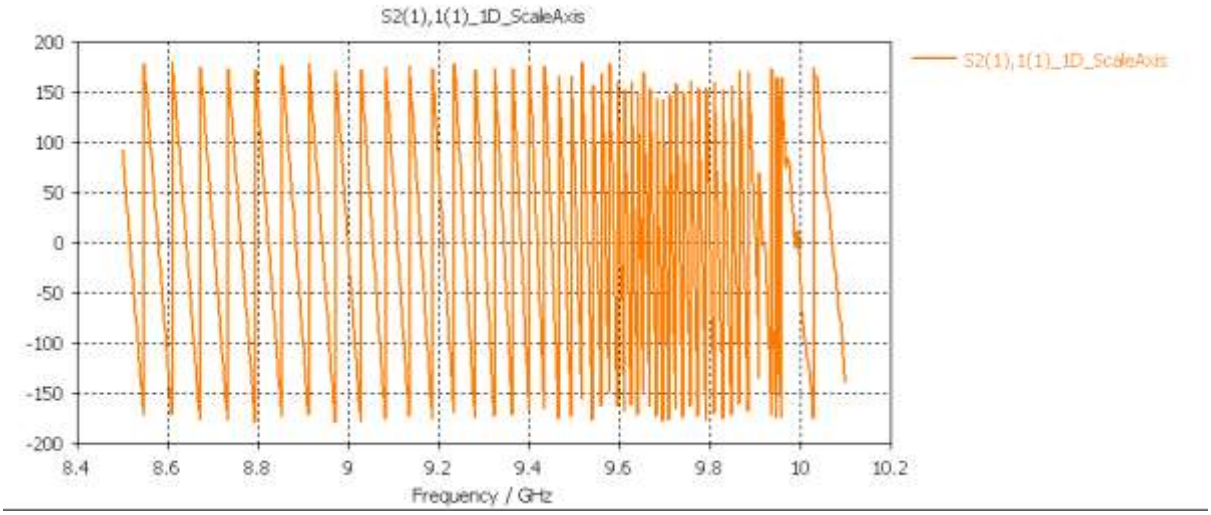

Figure 5 Phase information for the transmission S-parameter

As the phase shift associated with of a particular frequency at the output is dependent on its phase velocity, whilst the variation of the phase as a function of frequency is associated with the group speed, it is possible to calculate the dispersion of the pulse compressor.

3.1.3 Numerical Calculation of Dispersion using Eigenmode Solver

In addition to using the transient solver of CST Microwave Studio to calculate the dispersion, it is also possible to calculate the dispersion using the eigenmode solver. In this case the model consists of a single period as shown in figure 6. Scanning over a range of phase differences, from -180 degrees to 180 degrees, between the two ends of the waveguide the eigenmode solver finds the modes (and associated frequencies) which are valid solutions to Maxwell's equations, figure 7. From this it is possible to reconstruct the dispersion of the helical waveguide.

Distribution A Distribution Approved for Public Release: Distribution Unlimited

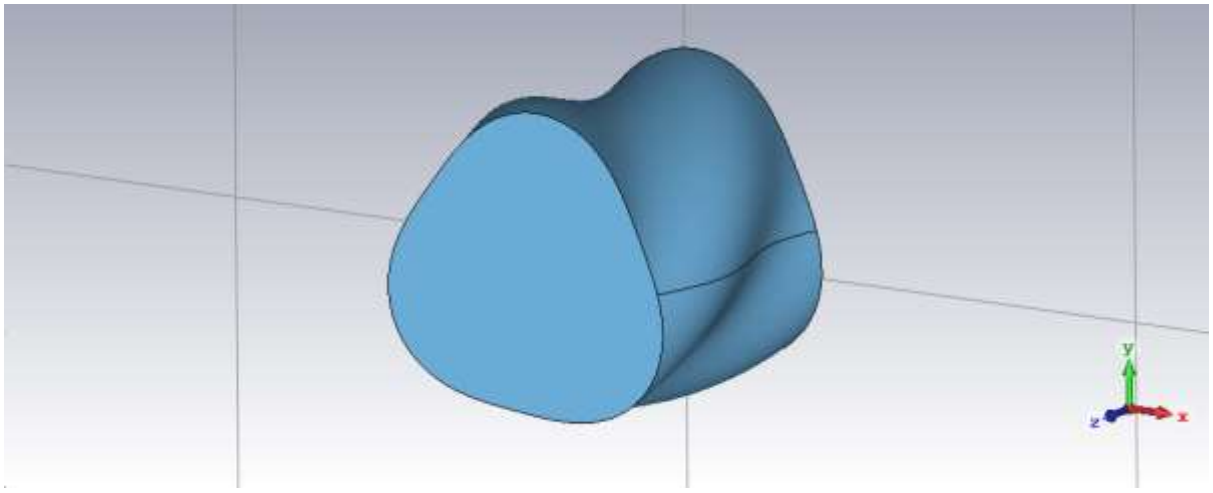

Figure 6 CST Microwave Studio model of single period of helical waveguide for calculation of dispersion using eigenmode solver

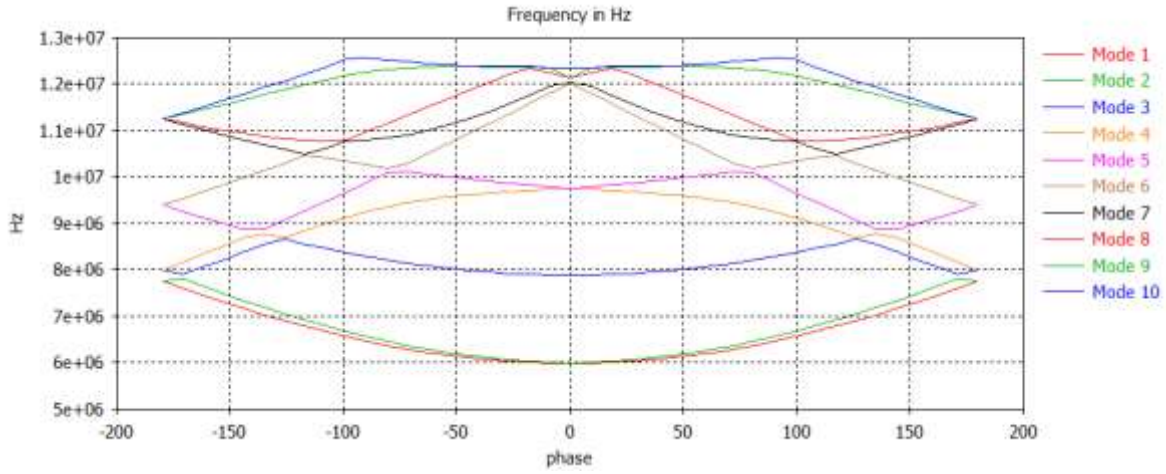

Figure 7 Solutions from eigenmode solver from which dispersion of helical waveguide can be calculated

3.1.4 Measurement of Dispersion of Pulse Compressor Using VNA

For the actual pulse compressor the best method for determining the dispersion is through direct measurement using a Vector Network Analyser. The dispersion is obtained directly from the phase information between ports 1 and 2.

Distribution A Distribution Approved for Public Release: Distribution Unlimited

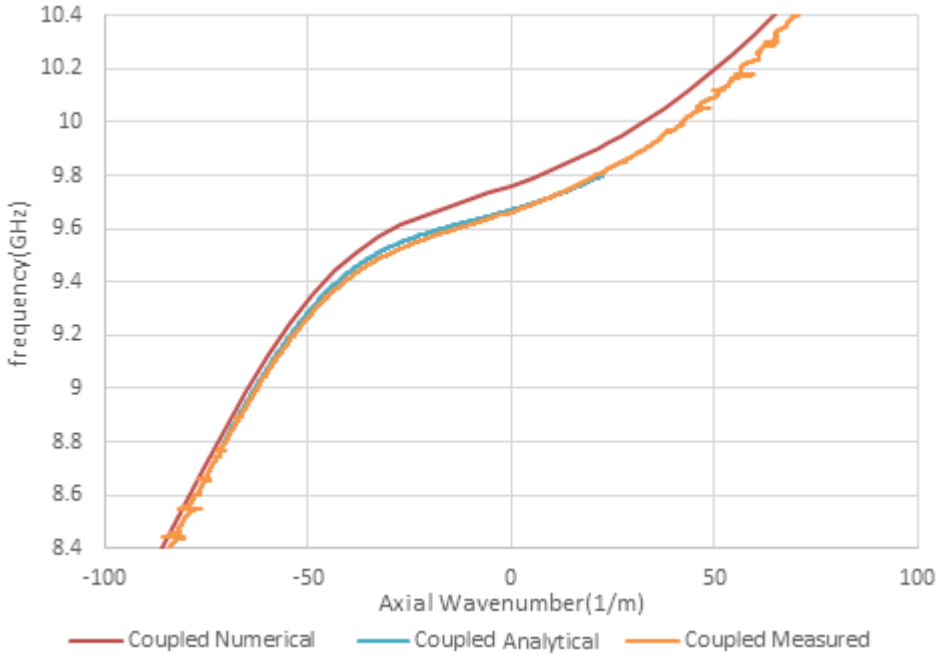

Figure 8 Dispersion for helical waveguide for coupled mode

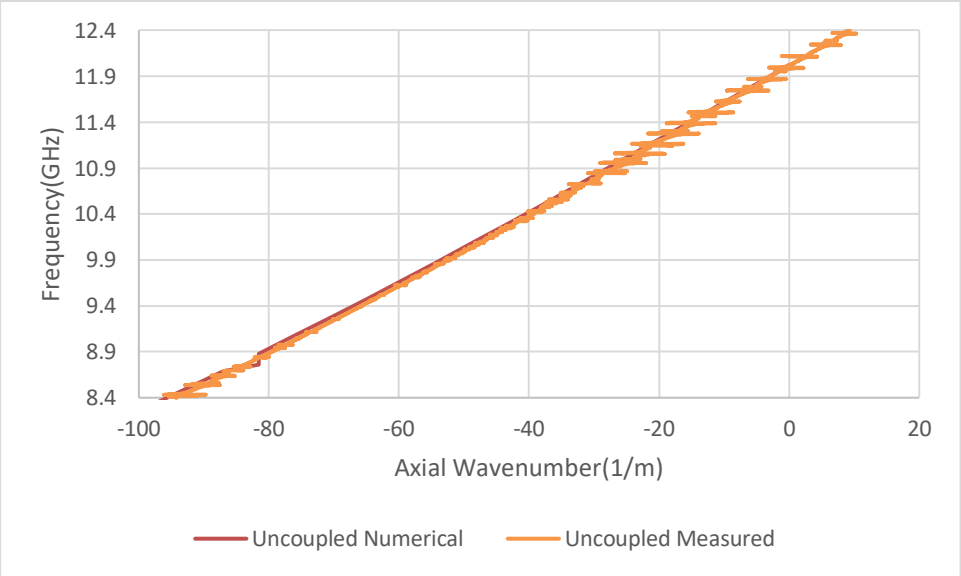

Figure 9 Dispersion for helical waveguide for uncoupled mode

Figure 8 shows the dispersion calculated analytically (section 3.1.1), numerically (section 3.1.3) and measured (section 3.1.4) for the coupled mode. Figure 9 shows the dispersion calculated numerically (section 3.1.3) and measured (section 3.1.4) for the uncoupled mode. There is good agreement between all methods apart from a slight discrepancy in the coupled mode dispersion by the numerical method. Note the small ripples evident in the wavenumber seen at regions above10 GHz and below 8.8

Distribution A Distribution Approved for Public Release: Distribution Unlimited

GHz are associated with the signal being out of the bandwidth of the circular polarising convertors used in the measurement apparatus.

3.1.5 Production of Input Pulse

Using any of the above methods results in a dispersion curve of the pulse compressor. As the group velocity is given by the derivative of angular frequency with respect to axial wavenumber then the variation of group velocity with frequency can be calculated, figure 10. Since the desire is for all frequencies in the input pulse to arrive at the output of the pulse compressor at the same time it is now possible to construct a chirping input pulse for the pulse compressor.

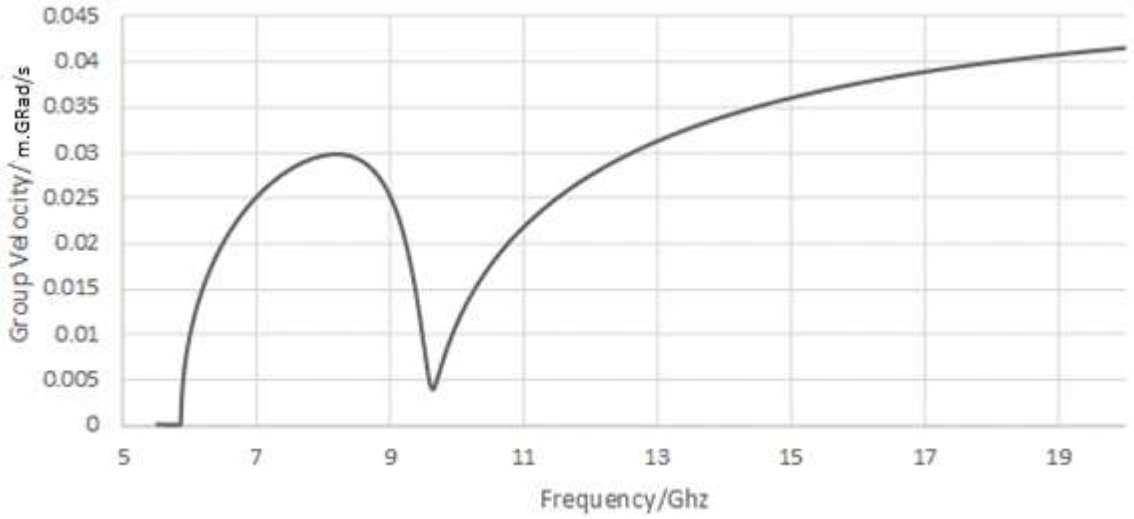

Figure 10 Group velocity as a function of frequency

As the input pulse needs to be in a region of changing group velocity and ideally where that rate of change is maximum there are three identifiable regions in figure 10 that are suitable, (1) from cut-off to 8.5GHz, (2) 8.5GHz to 9.5GHz and (3) greater than 9.5GHz. Region 1 is similar to a smoothbore waveguide with the associated problems. In Region 3 higher order modes exist and are shown to be excited both by the simulations and by measurement, which seriously affects the compression of the pulse. Region 2 is the most desirable region with its particularly steep slope.

Distribution A Distribution Approved for Public Release: Distribution Unlimited

3.2 Time Domain Simulations of Pulse Compressor Performance

3.2.1 Analytic Input Pulses

The first set of simulations of the pulse compressor used the model in figure 2 and were run with the waveguide walls made of a perfect electrical conductor, and therefore had no losses. It should also be noted that whilst the launched wave is linearly polarised there is no elliptical convertor on the output and therefore the output signal is circularly polarised. The output of the model however is based on two orthogonal linearly polarised modes, so the power is split equally between the two modes and therefore each mode carries half the power of the compressed signal. It should be noted that because the signals shown in figure 11 show amplitudes (power goes as the square of the amplitude) the energy pulse compression is much greater than the visual impression indicated in figures such as figure 11.

An input pulse chirp was calculated for the pulse compressor shown in figure 2 using the analytical method for predicting the dispersion and used to inject energy into the pulse compressor model. Figure 11 shows the input pulse (red) and the output of one of the linear polarisations (brown). As can be seen the amplitude compression factor is around 3.5, and of course the signal in the output is split across two linear polarisations, whereas in the input the signal is entirely associated with a single linear polarisation. To estimate the total compression factor one must double the apparent power compression factor (given as the square of the amplitude compression factor). This is shown in figure 12.

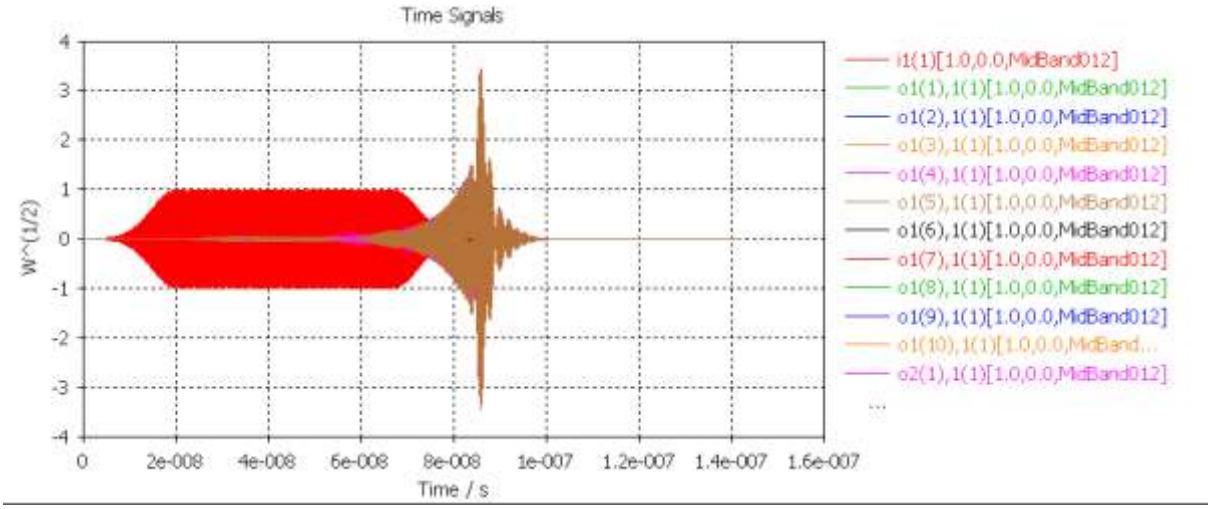

Figure 11 Pulse compression of input pulse calculated using 53 periods

Distribution A Distribution Approved for Public Release: Distribution Unlimited

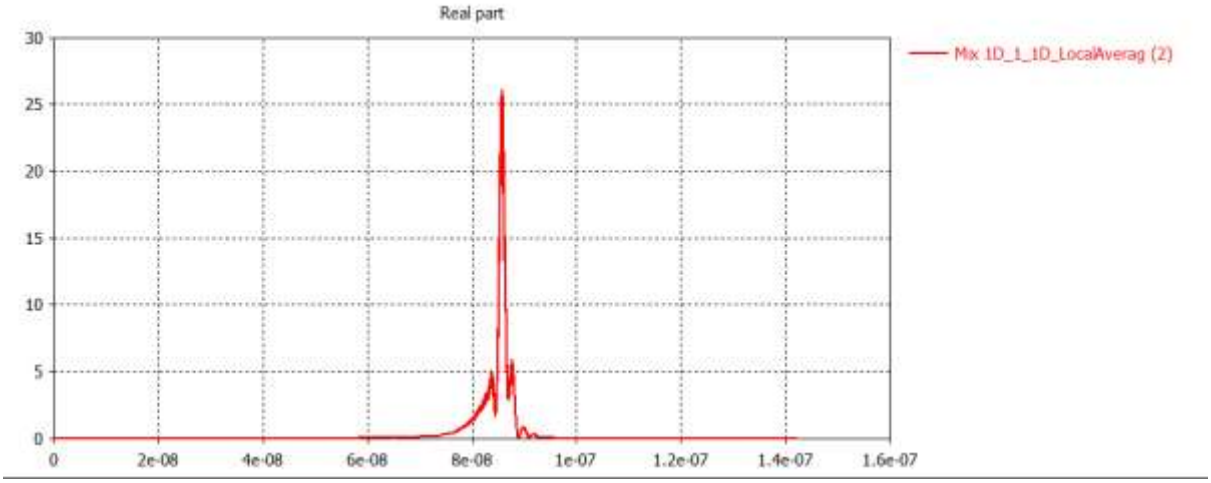

Figure 12 Amplification factor of output pulse

3.2.2 Numerically Calculated Input Pulse

A second method was developed to synthesise an optimal input chirp signal for the pulse compressor. This consists of passing a Gaussian pulse over the desired frequency range through the pulse compressor and from that calculating a suitable input pulse. The resultant output pulse is shown in figure 13. Figure 14 shows that although this pulse produces a good match a compression of just under 18 is achieved, not as good as that achieved with the analytical approach as shown in figure 12. This method however does have the 'in principle' benefit of allowing the input pulse to account for the full diversity of components in the compressor assembly. Additional investigation of this method should allow it to predict an input chirp which should exceed the performance of that predicted by the analytical method.

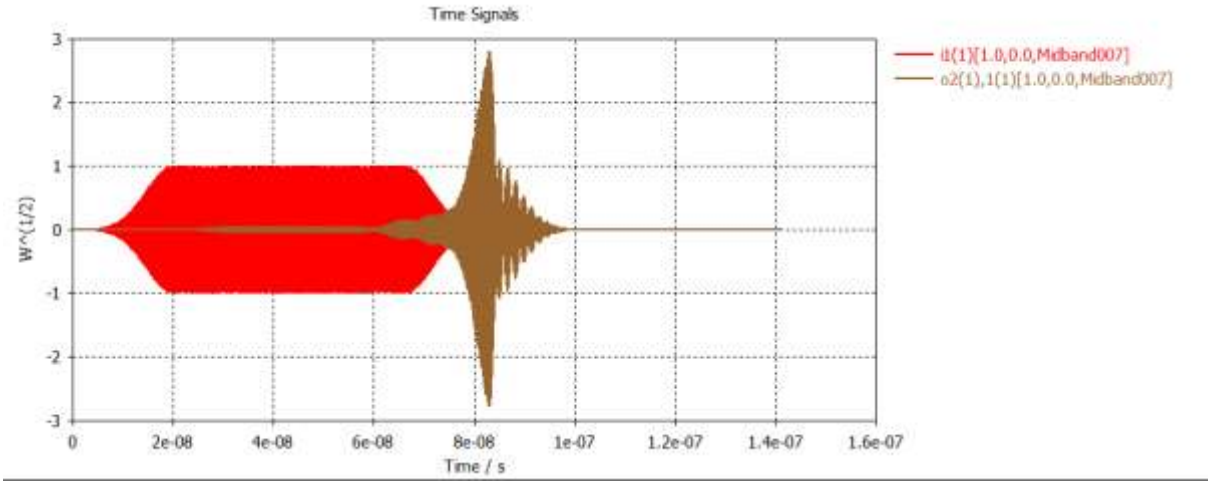

Figure 13 Numerically calculated input and resultant output pulse

Distribution A Distribution Approved for Public Release: Distribution Unlimited

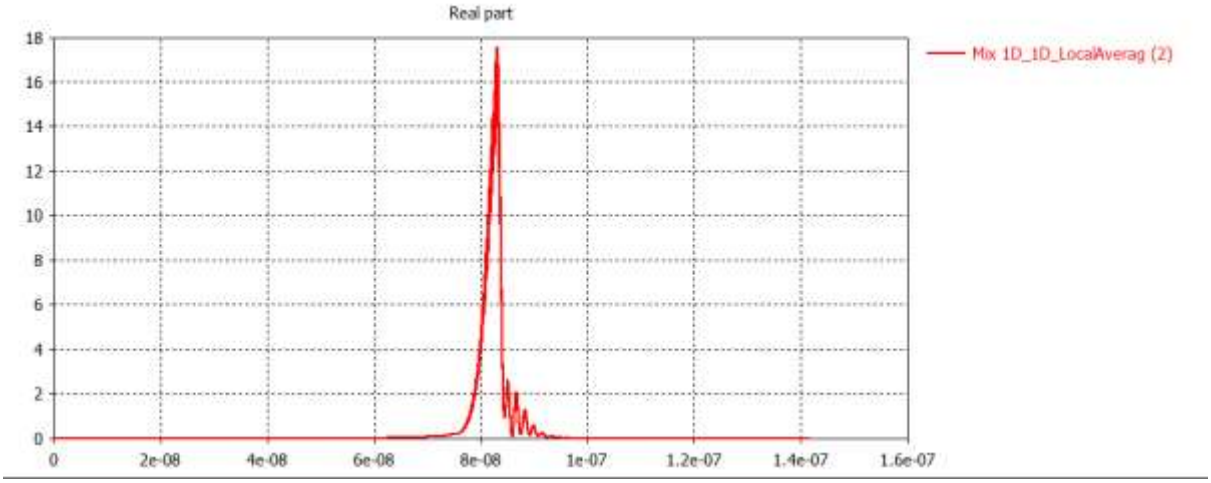

Figure 14 Pulse compression factor for numerically calculated input pulse

3.2.3 Copper waveguide simulations

Simulations in sections 3.2.1 and 3.2.2 used a perfect electrical conductor as the waveguide material. Simulations were run replacing the perfect electrical conductor with copper to see the effect a lossy metal has on the pulse compression. The results are shown in figure 15 and figure 16. There is little change in the shape of the output pulse indicating there is no distortion of the output pulse due to the presence of the copper waveguide, however there is a drop in the pulse compression factor of about 15%.

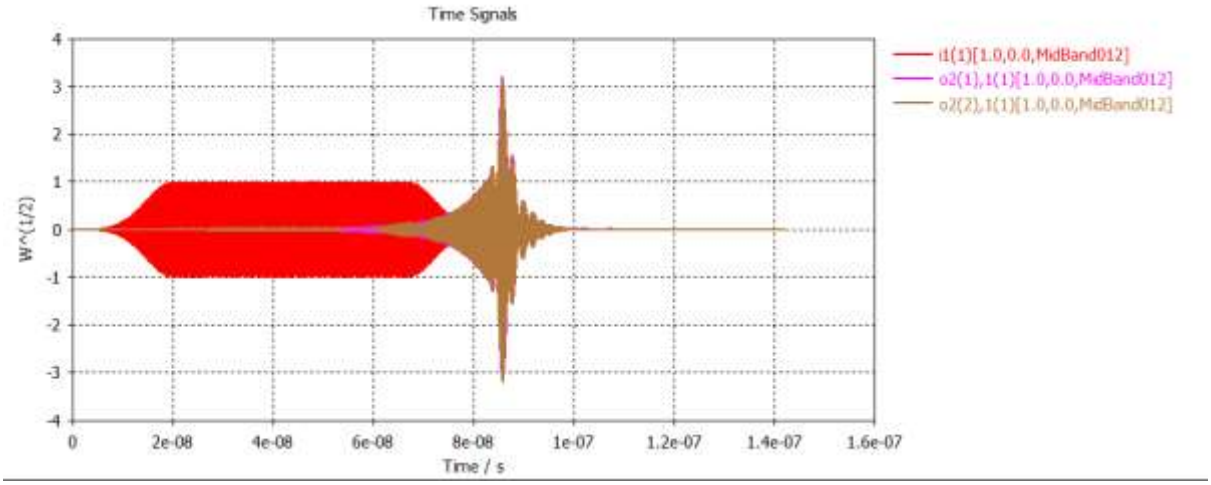

Figure 15 Analytical input pulse and output pulse with copper waveguide

Distribution A Distribution Approved for Public Release: Distribution Unlimited

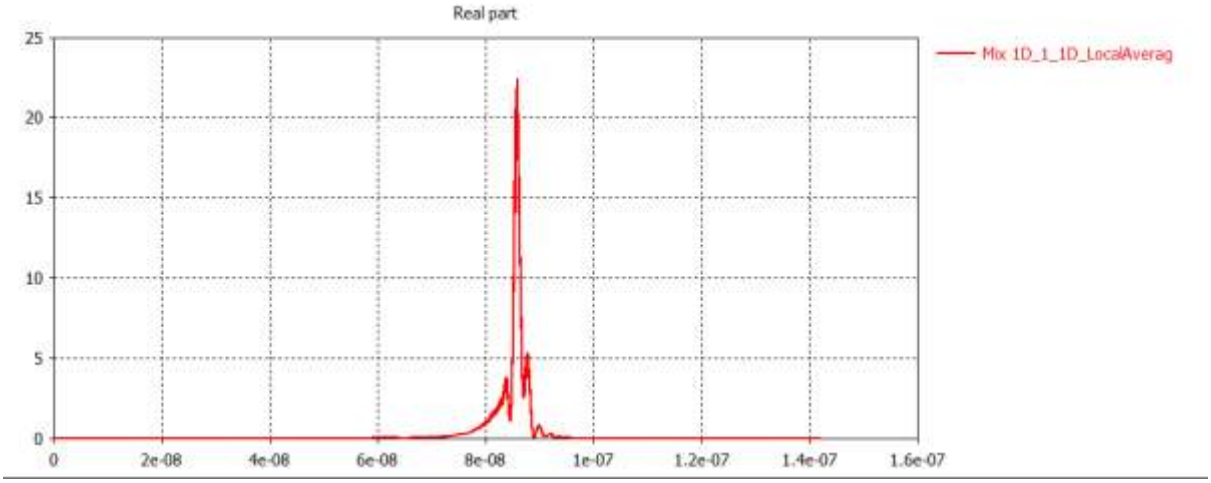

Figure 16 Pulse compression factor for analytically calculated input pulse with copper waveguide

3.2.4 Power Handling Simulations

With high power microwave devices there are two primary effects that put an upper limit on the maximum power they can handle. The first is power loss due to resistance of the waveguide material. Obviously, if the power loss to the waveguide is too high then the waveguide may be subject to thermal load (essentially from resistive heating) which could result in physical damage to the waveguide. If the waveguide is operating under vacuum conditions (sometimes done to prevent arcing of the fill gas) then it is also possible that gasses absorbed on the wall will be evaporated into the volume bringing enhanced risk of breakdown due to this thermal heating effect. The thermal heating effect is a function primarily of the average power being carried by the waveguide. In the present case even with potentially rather high peak power, it is not expected that the duty will be so high that the average power would exceed the power handling in the fundamental mode of the rectangular waveguide at these frequencies (300kW average for WG16 standard X-band waveguide in air at standard pressure and temperature). The corrugated waveguide is formed of similar materials, of similar (or greater) thickness as single mode rectangular waveguide, and also operates far from cut-off in the operating mode. Unlike many dispersive waveguide structures it is relatively large and features typically only relatively robust copper walls with no dielectrics or isolated features. Hence it can be reasonably expected that the average power handling capability will be comparable to that of normal waveguide, which is not expected to prove a significant limiting factor for applications. The other limitation

Distribution A Distribution Approved for Public Release: Distribution Unlimited

arises from the very high electric fields which can cause breakdown in the device. In dry air at 1 atmosphere the breakdown voltage is 3MV/m. Using information from the model it is therefore possible to estimate the maximum power of the input signal and the maximum output power.

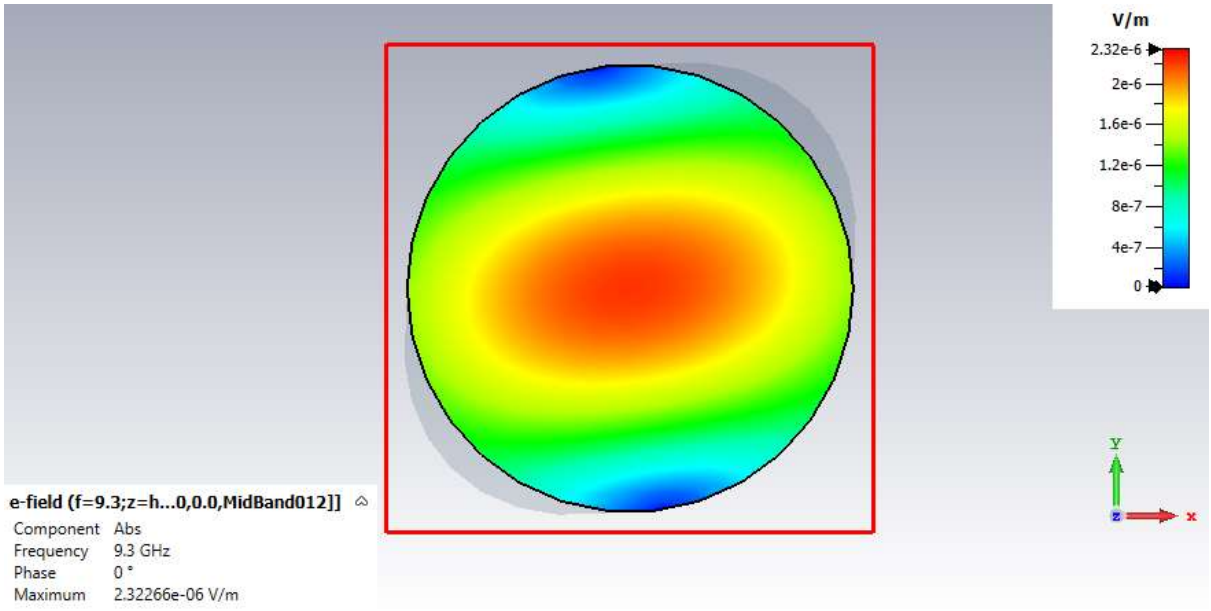

Figure 17 Electric field in smoothbore waveguide

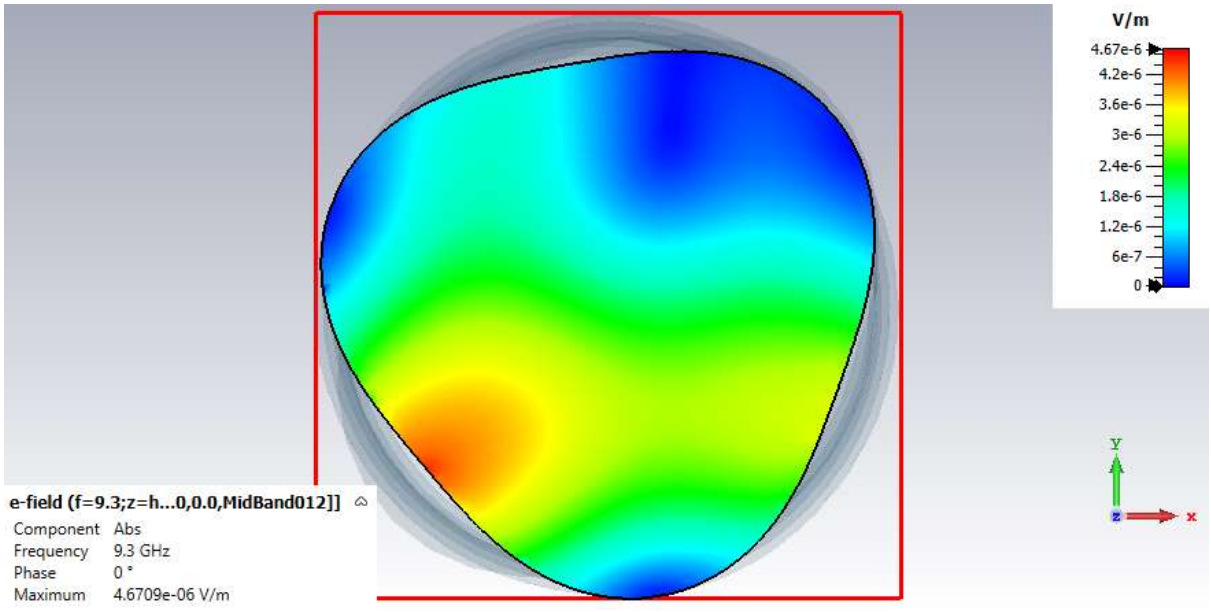

Figure 18 Electric field in helical waveguide at the same signal level as figure 17.

The electric field in the helical waveguide will experience enhancement due to the geometry of its cross-section (this is true even for ideal surfaces). From figure 17 and

Distribution A Distribution Approved for Public Release: Distribution Unlimited

figure 18 it can be seen that for the same input power, the peak field in the helical waveguide is approximately double that of the smoothbore waveguide. Therefore the maximum field in the smoothbore section must be 1.5MV/m so that the field in the helical section is no greater than 3MV/m.

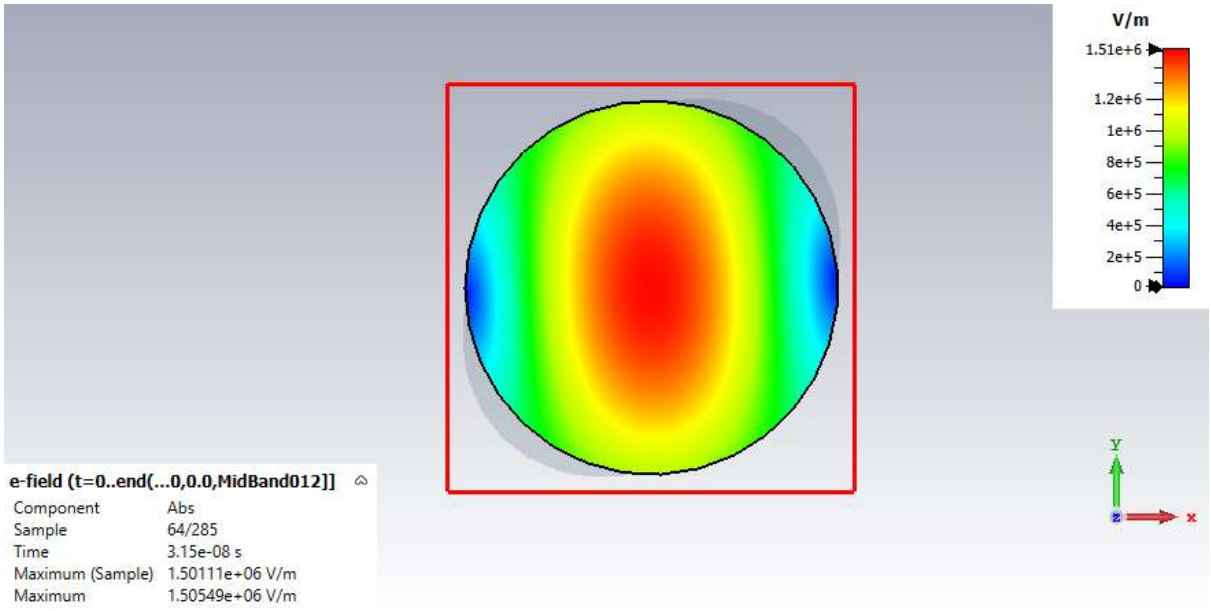

Figure 19 Electric field in smoothbore waveguide with power of 1.3MW.

Building on this analysis the maximum output power that this pulse compressor in dry air at 1 atmosphere can support is 1.3MW, and since the power compression factor is approximately 25, the maximum input power would appear to be limited to approximately 50kW. We should however note that this very high E-field level would only arise at the output end of the compressor where the pulse duration is very short- this can significantly mitigate the risk of breakdown, data presented in[x] shows that the holdoff behaviour for short unipolar pulses and RF pulses is in close alignment. For pulses of a few ns in duration (as will be the case towards the output of the pulse compressor) the breakdown field strength would be above 6MV/m in dry air at 1 bar. This would raise the peak output power levels which may be sustained to 5.2MW and input power levels of 200kW. In terms of wideband tubes this sort of power level implies gyrotron travelling wave amplifiers.

This can be further improved by either having the pulse compressor in vacuum or pressurised, possibly using a suitable gas such as SF_6, however care has to be taken in the transition back to air to ensure that the transition (always a weak point in any

Distribution A Distribution Approved for Public Release: Distribution Unlimited

system is not at risk of flashing over). This can be readily achieved by tapering the circuit up to a large diameter before performing the transition back to air for coupling to the antenna. Alternatively one may use an antenna assembly immersed in a 'gas bag' radome- moving the delicate transition to air to a location somewhat distant from the antenna where the field is sufficiently low that the air is not at risk of arcing.

In vacuum the ultimate limitation is the field at which the material of the walls can explosively sublimate. To first order this may be estimated from the Kilpatrick criterion[xi], at ~ 10MV/m, corresponding to peak power levels that may be sustained in a three-fold compressor of around 14MW implying input power levels of around 560kW. However here we deal with relatively short duration pulses (even the input pulse is measured in ~ 50 ns). If we assume a relatively long relaxation period between the pulses, analysis of short pulse breakdown associated with 3cm wavelength radiation indicates that the limiting field strength for such pulse durations might reach as high as 50MV/m [xii]. In pulsed vacuum breakdown, the tolerable pulse amplitude increases as the pulse duration shrinks due to the time required for explosive sublimation of field emission sites. In a pulse compressor, the field amplitude grows as the inverse of the square root of the pulse duration- it therefore seems reasonable to assume that if the system will be able to carry the input pulse that it will also be able to carry the output pulse. 50MV/m would imply power levels in excess of 100 MW can be carried at the input to the structure, with compressed pulses exceeding a few GW possible.

It is also attractive to consider a pressurised or electronegative gas fill. Pressurisation to 4 atmospheres dry air will lead to an increase in the breakdown field strength in air (for long pulses) to 100kV/cm- corresponding to an order of magnitude uplift on the power capability compared to air at 1 atmosphere. It is likely that there will be further enhancement due to the relatively short duration of the signal pulse. This corresponds to a peak power level capability exceeding 13MW with an input signal of around 500kW- without allowing for the short pulse uplift.

Electronegative gasses are highly beneficial in suppression of breakdown. Even a small fraction of such a gas added to a background of nitrogen will significantly uplift the tolerable peak electric field amplitude. Pure SF_6 at 2 atmospheres (absolute) will uplift the power handling by a factor of 37 compared to dry air at one atmosphere [xi].

Distribution A Distribution Approved for Public Release: Distribution Unlimited

This would correspond to 48 MW peak output power and an input power of almost 2MW. Greater pressurisation will produce further increases in performance.

In practice the peak power performance in pressurised and electronegative gas is likely to significantly exceed these estimates due to the short duration of the pulse. Additional data would be required on the short pulse AC breakdown behaviour of gasses in these conditions.

It is relevant to note here that the focus on 3-fold compressors was determined by the focus on exploring spectral flexibility. 5-fold pulse compressors for the same spectral range comfortably support multi-GW levels of power in vacuum, however it is not likely that these can operate, or be combined with other critical required components to operate, over more than a very limited optimum spectral range..

3.3 Alternative Circular Polariser Design

The polarising element is used to convert a signal between linear polarisation and circularly polarisation. The input signal may be described as a superposition of two degenerate, orthogonal, linear polarised signals in circular waveguide. The simplest approach exploits an elliptical deformation of the waveguide, with the major and minor axes aligned at 45^{o} to the plane of polarisation of the incoming dipole mode. Each of these orthogonal linear polarised signals experiences different group and phase velocities as they travel through the convertor and therefore the phase between the components will change. If the signals acquire a phase difference of $m \cdot 180^{o}, m \in \mathbb{Z}$, then the signal is linearly polarised at 45 degrees to the elliptical convertors axes. If the phase difference between the two signals is $(m+1) \cdot 90^{o}, m \in \mathbb{Z}$, then the signal will be circularly polarised. Any phase difference between these will result in a varying degree of elliptical polarisation, a superposition of linear and circularly polarised signals. To convert from linearly polarised to circular the axes of the elliptical convertor are placed at 45 degrees to the polarisation of the input signal, and similarly to convert from circular to linear polarisation the elliptical convertor axes should be 45 degrees to the desired polarisation output.

Most of the measurements reported here were obtained using the simplest polarising convertor as illustrated below. The bulk of the elliptical convertor is a smooth transition from the circular cross-section to the elliptical cross-section and back, figure 20. As

Distribution A Distribution Approved for Public Release: Distribution Unlimited

stated above the major axis of the elliptical cross-section is aligned to be 45^{o} with respect to the input mode polarisation. The component of the input signal whose wavevector is aligned with the major axis of the ellipse will have a higher group velocity, and lower phase velocity than the component of the input signal aligned with the minor axis.

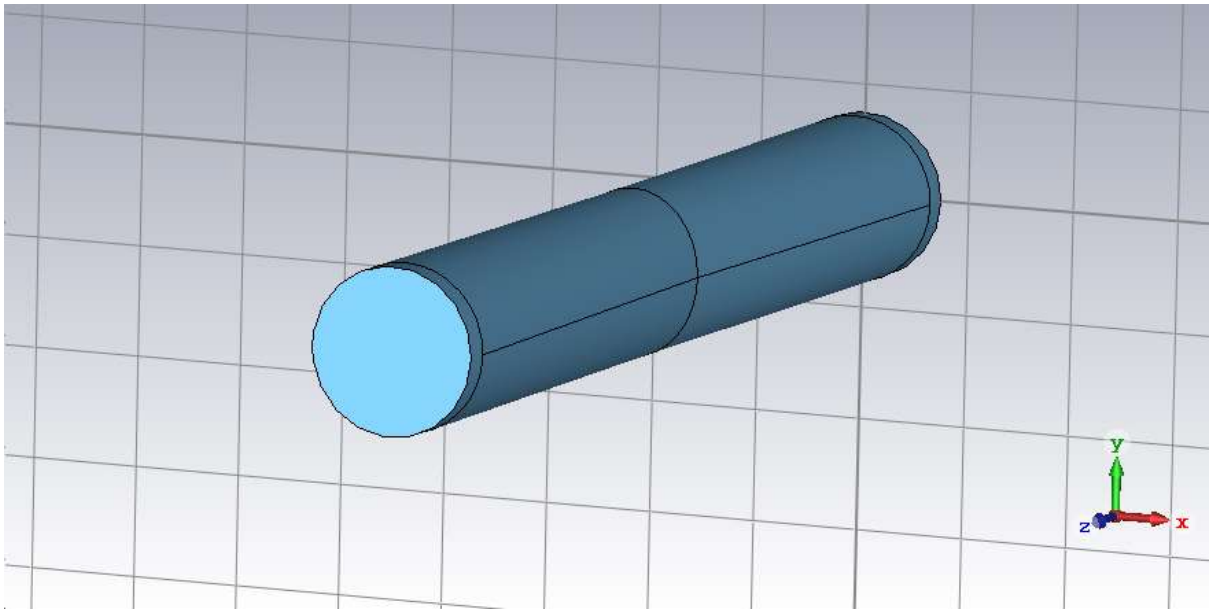

Figure 20 Circular polariser using elliptical cross-section at centre

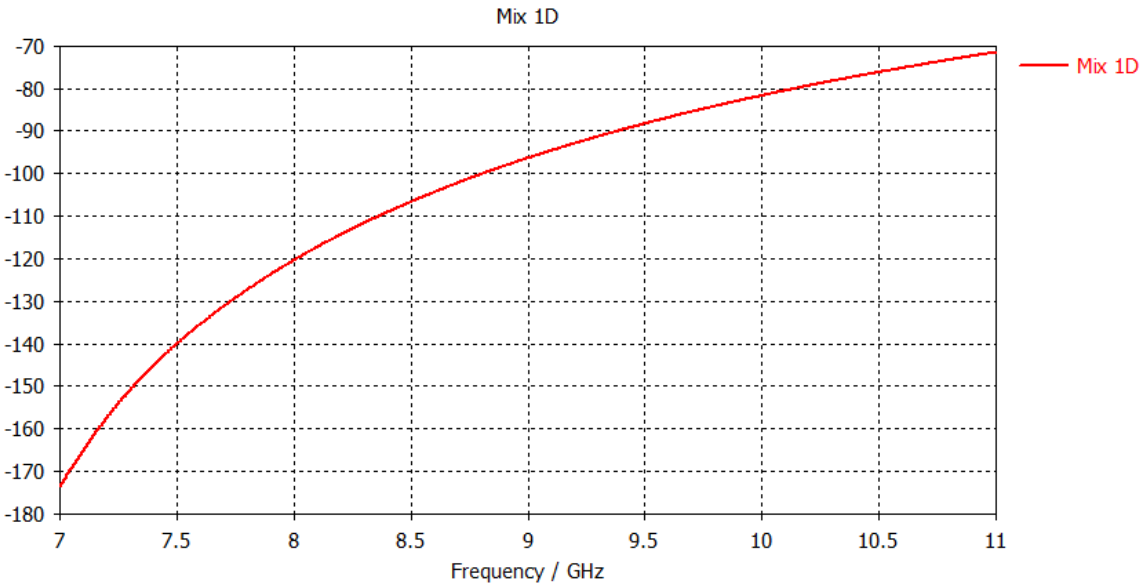

Figure 21 Phase versus frequency for simplest polariser using elliptical cross-section at centre

Distribution A Distribution Approved for Public Release: Distribution Unlimited

As can be seen from figure 21 the phase change is dependent on the frequency and this limits the frequency range that the elliptical convertor can be used over. The particular circular mode convertor calculated in figure 21 was designed to allow testing of the helically corrugated waveguide above the optimum frequency range and is hence centred on 9.5GHz. Two components were fabricated and tested as described in section 2 (by taking the difference of the phase shift observed for the two different polarisations). The results of the experimental measurements are shown in figure 22.

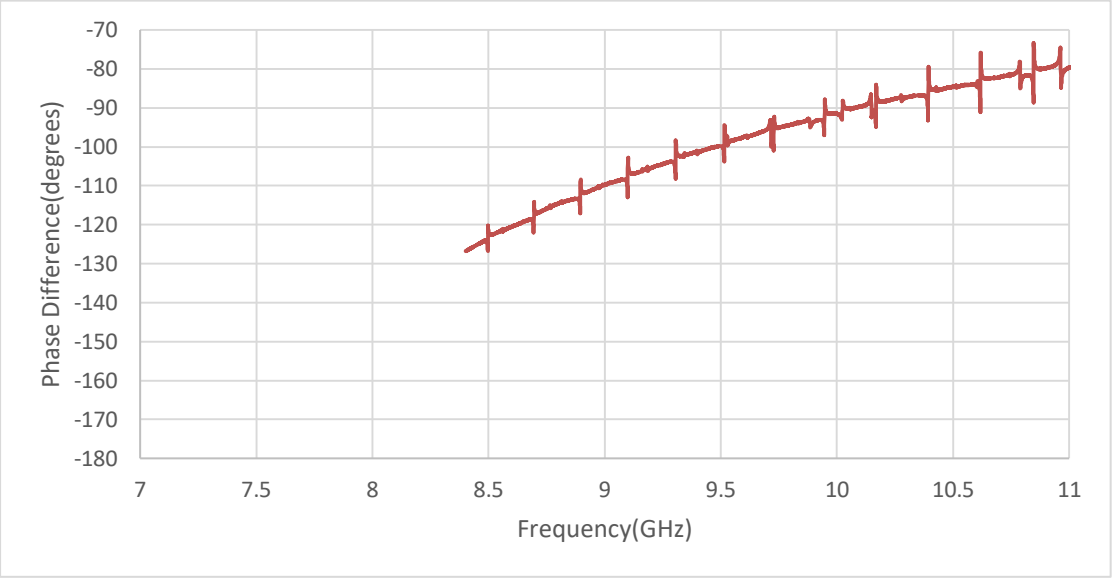

Figure 22 Measured phase versus frequency for simplest polariser using elliptical cross-section at centre

The chirp range of a pulse compressor of this type is typically $\pm 2.5\%$ of the central frequency and it can be seen that there is meaningful variation in the purity of the circularly polarised signal over such a bandwidth, with a variation of order $\pm 5\%$ in phase (although this is a significant function of the frequency). This in practice proves to be an acceptable level of variation. However if the pulse compressor is to be exploited across a wider spectral range then this variation could become problematic.

Another design for the polarisation convertor has been investigated which significantly enhances the overall bandwidth over which the convertor effectively excites the desired circularly polarised mode with a high degree of mode purity. This approach is still based on considering the signal to be composed of two components, but instead of an elliptical deformation in a nominally cylindrical waveguide the degeneracy is

Distribution A Distribution Approved for Public Release: Distribution Unlimited

broken by a periodic loading in one wall of a square waveguide, figure 23. A component based on this design has been subject to experimental test to verify the expected high performance of this novel polariser, see figure 24

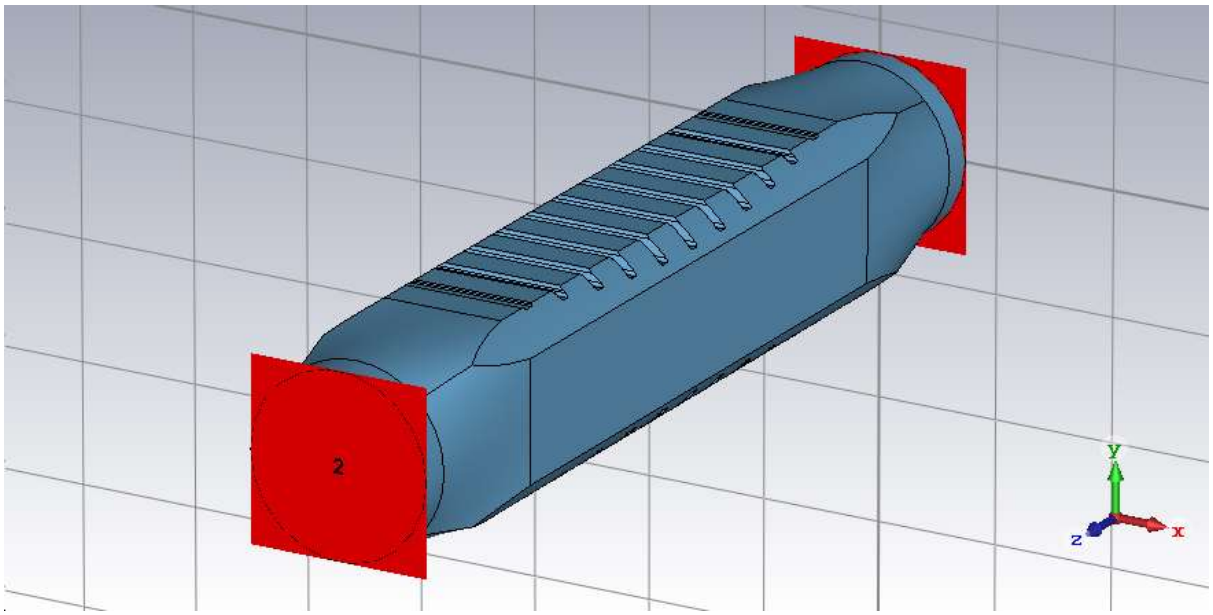

Figure 23 Circular polariser using periodic corrugation

Figure 24 Comparison of corrugated and elliptical approaches to the circular polariser

Distribution A Distribution Approved for Public Release: Distribution Unlimited

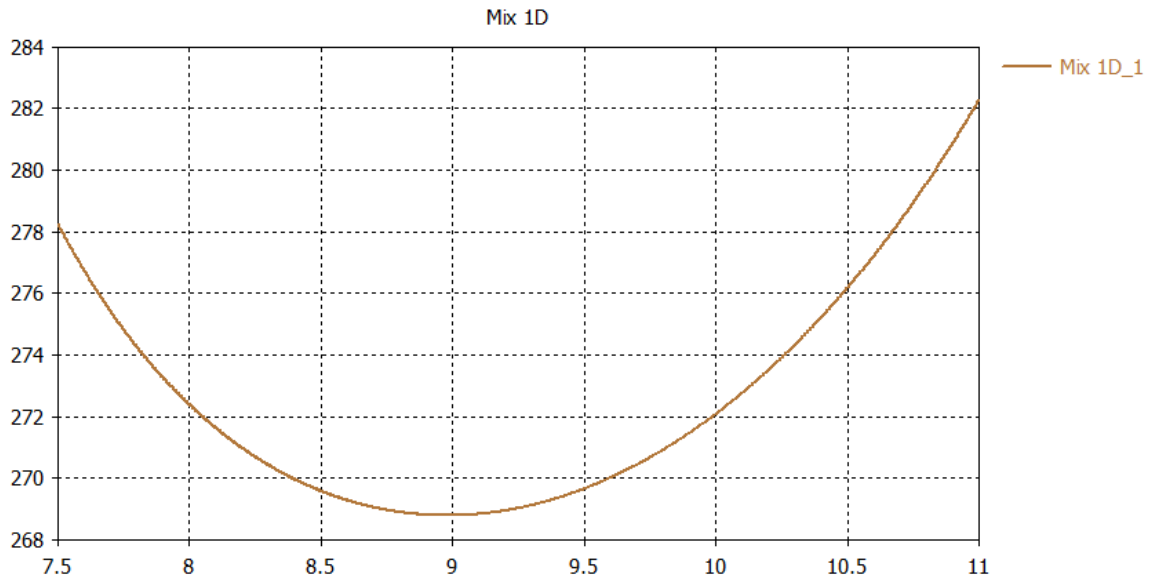

Figure 25 Phase versus frequency from circular polariser using periodic structure

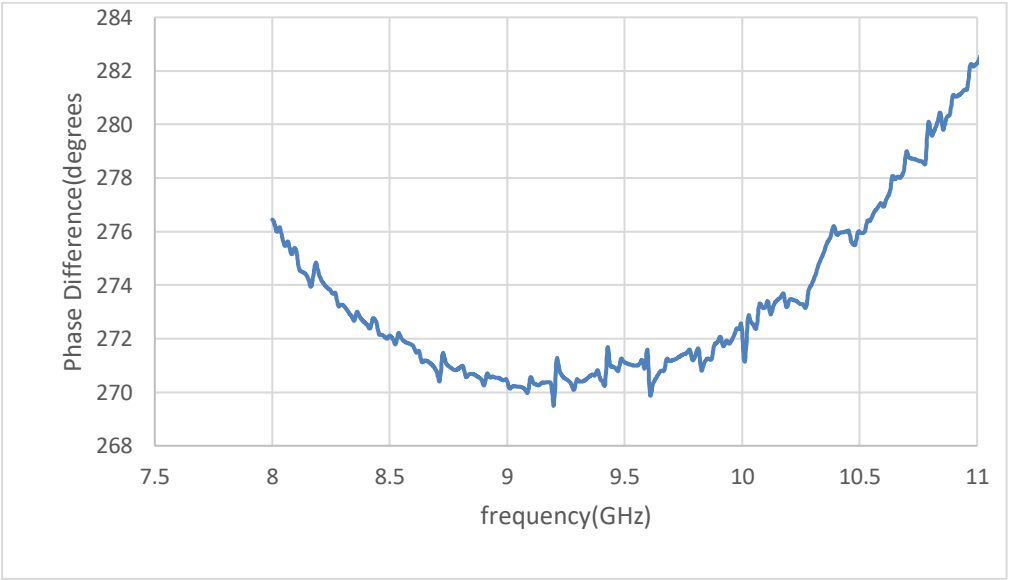

Figure 26 Measured phase vs frequency from circular polariser using periodic structure

Comparing figure 21 and figure 25 it can be seen that the periodically loaded structure has a significantly greater bandwidth. Assuming a phase difference of plus or minus five percent is acceptable the convertor with the elliptical cross-section operates from 9.1GHz to 9.7GHz, whilst the corrugated convertor operates from 7.3GHz to 10.3GHz. This innovation will be important to enable the deployment of a pulse compressor able to function over a wider spectral range in terms of the signal centre frequency. Figure

Distribution A Distribution Approved for Public Release: Distribution Unlimited

26 shows that the fabricated component does deliver the expected higher degree of polarisation purity over a wide bandwidth.

3.4 Double Pulse Compressor

The bandwidth of the pulse compressor is dependent on its dispersion, but is ultimately limited by the necessity for a strong frequency dependence of group velocity. It is not straightforward to extend this range. One attractive approach is to use the upper knee of the dispersion with an opposite chirp in the input signal, this is the range above 9.5GHz in figure 10. However in this range energy is readily scattered into alternative modes, including the orange 'upper' solution to the corrugated waveguide shown in figure 4. Many of these modes have a low group velocity producing an effective stopband where the energy is not effectively transmitted by the waveguide. It is certainly possible to make use of the region close to the cut-off of the dipole mode, as the frequency drops towards 6GHz in figure 10. However this has no advantages (and indeed significant disadvantages) over smooth waveguide pulse compressors. It may however be possible to effectively double the operating range of the pulse compressor by using two pulse compressors in series and by exploiting the relationship between dispersion experienced by the pulse and the handedness of the circular polarisation.

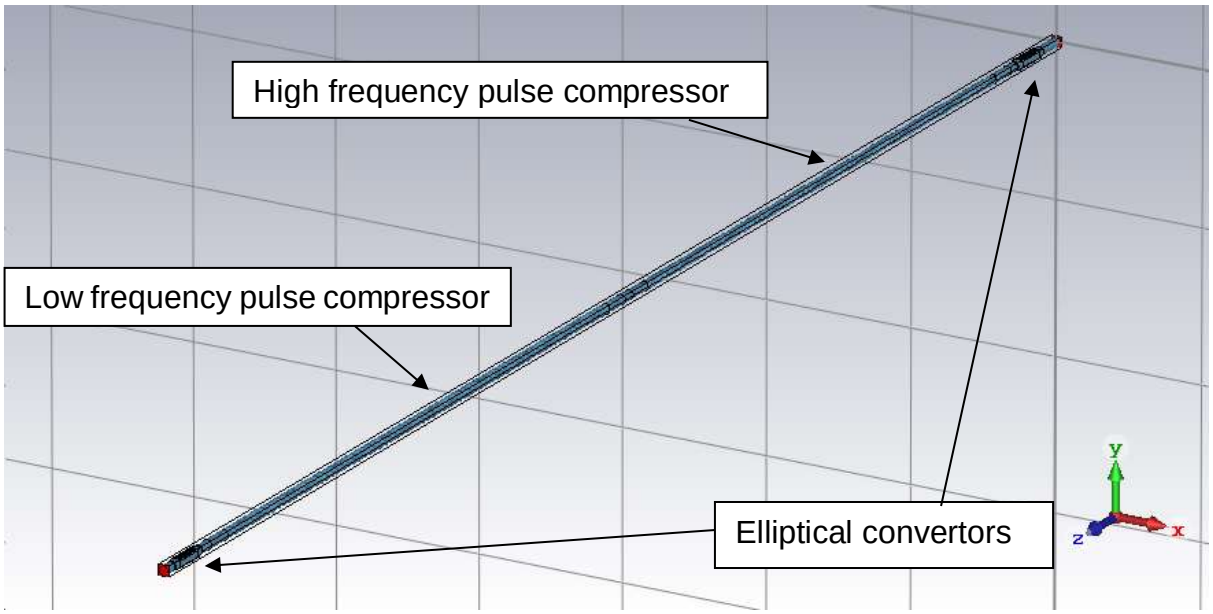

Figure 27 Double pulse compressor

Distribution A Distribution Approved for Public Release: Distribution Unlimited

Figure 27 shows the numerical model of the “double” pulse compressor. The corrugated polarisation convertor is used due to its superior bandwidth. A second polarisation convertor has been positioned at the end of the model to convert the circularly polarised radiation back to linear. The geometry of the two pulse compressors has been adjusted to optimise them for two adjacent spectral bands. It is not strictly essential that the two bands be adjacent, although they also cannot be arbitrarily separated, primarily since the lower frequency compressor must operate at a frequency which is not too close to the cut-off of the higher frequency device. A linearly polarised signal designed to interact with the higher frequency pulse compressor (9 to 9.6GHz) has its axis rotated 45 degrees relative to the y-axis and a linearly polarised signal designed to interact with the lower frequency pulse compressor (8.5GHz to 9GHz) has its axis rotated minus 45 degrees relative to the y-axis (i.e. the two input signals are simply injected polarised perpendicular to each other). In practice several schemes exist which can simultaneously or separately excite each of these modes, the simplest being a double sidewall coupler type scheme. When these pulses pass through the polarisation convertor they respectively excite two counter rotating pulses. Because of the chirality of the system, the signal designed for the lower frequency compressor passes through the higher frequency convertor in the ‘wrong’ circular polarisation. This mode has a dispersion very close to that of a smooth waveguide and the signal therefore has a very high group velocity and suffers little dispersion and only modest attenuation. When the signal passes through the lower frequency compressor it is subject to effective pulse compression.

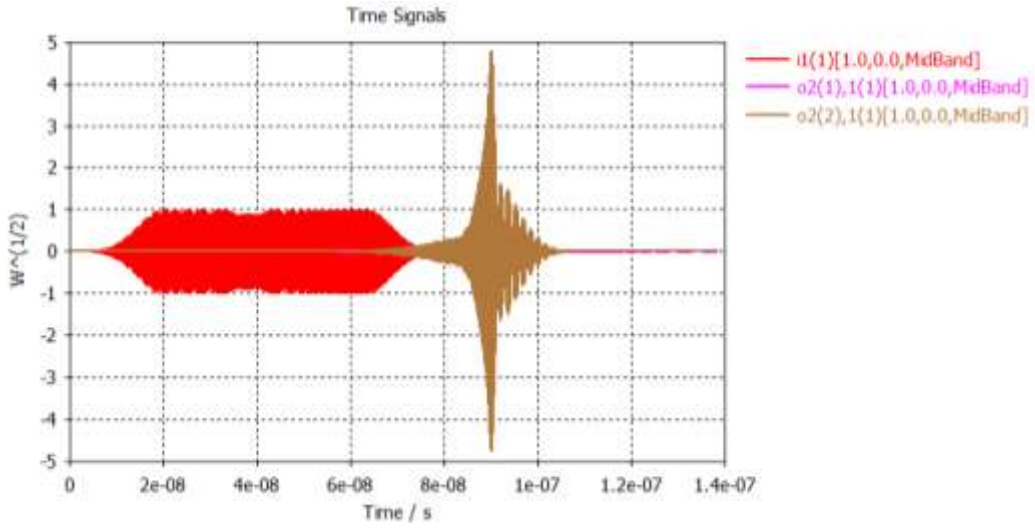

Figure 28 Port signal of high frequency input signal in double pulse compressor

Distribution A Distribution Approved for Public Release: Distribution Unlimited

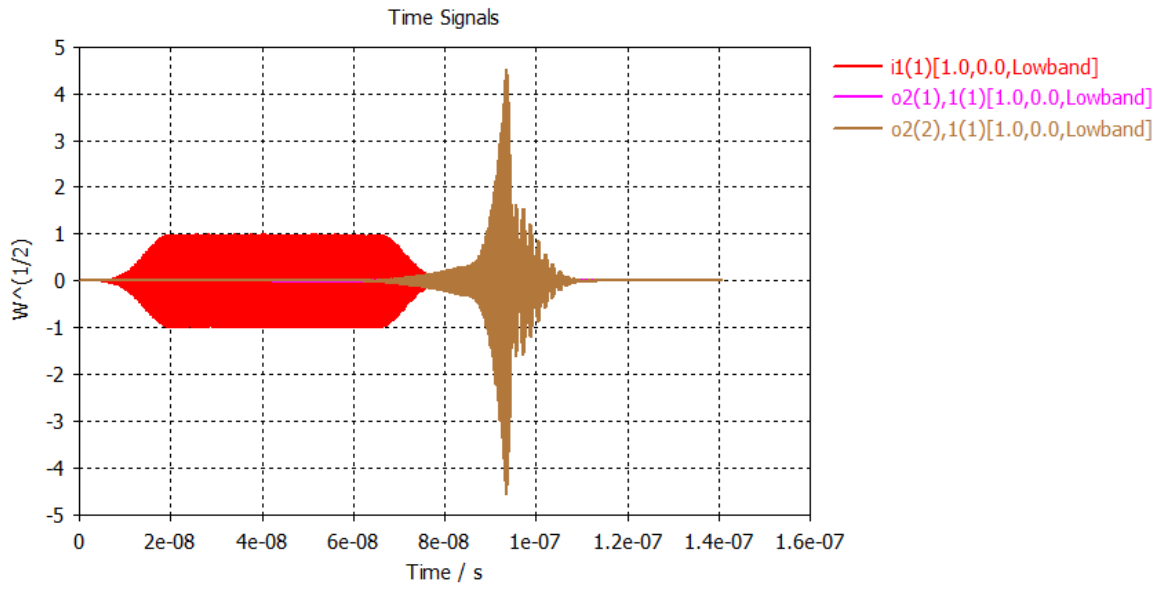

Figure 29 Port signal of low frequency input signal in double pulse compressor

Broadly the same effects apply to the higher frequency signal, however here the chiral asymmetry of the dispersion behaviour is even more important. Whilst the low frequency signal would have passed through the high frequency compressor with limited dispersion even in the coupled mode (see the range below 9GHz in figure 10 where the signal has only a modest variation in group velocity), the high frequency signal would have been blocked by the stopband in the low frequency compressor. However the stopband does not exist for the counter-rotating wave which is not effectively coupled by the corrugation, see the dispersion described in figure 9 which shows the uncoupled mode is almost dispersionless across the entire spectral region. Therefore the high frequency signal can propagate through the compressor tuned for the low frequency signal without perceiving the corrugation. Input pulses using the numerical method outlined in section 3.1.2 for each pulse compressor were used and the results of passing these two pulses independently through the double pulse compressor are shown in figure 28 and figure 29. They verify that each pulse can be compressed by this structure. The higher frequency pulse arrives at the output at 9ns, while the lower frequency pulse has a slightly lower group velocity due to being closer to cut-off throughout the compressor and arrives at the output at 9.35ns. This would need to be corrected for in the input if it were desired that the two signals be launched at the output simultaneously (but this is relatively straightforward to do).

Distribution A Distribution Approved for Public Release: Distribution Unlimited

3.5 Preliminary U-bend Study

The current pulse compressor is relatively compact, being only a few cm across, however it does extend to some two metres in length. The double pulse compressor would extend to 4m at X band. An investigation was started to establish if the pulse compressor designs could be folded to make them more compact. This would require having two sections of the helical waveguide, both sections bookended with tapers to smoothbore waveguide, and having a U-bend in the waveguide. Since the pulse in the compressor is circularly polarised, and it is likely that the E-plane and H-plane components of the signal will perceive the bend in the waveguide differently, it is important to establish if the U-bend in any way distorts the signal. The first step of this process was to check what happens to a linearly polarised signal, polarised in the plane of the bend and in the orthogonal polarisation. An initial bend with radius of 44.1mm (3 times waveguide radius) was chosen and the results are shown in figure 30 and figure 31, where the signal input, port 1, is the lower of the ports and the output is the higher of the ports, port 2.

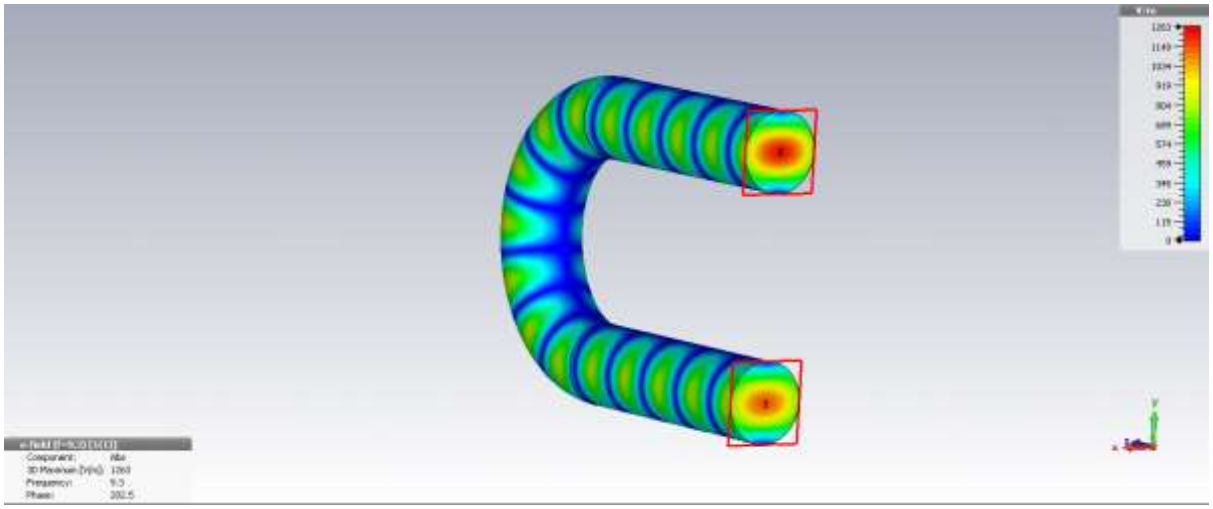

Figure 30 44.1mm radius U-bend with horizontal linearly polarised signal

Distribution A Distribution Approved for Public Release: Distribution Unlimited

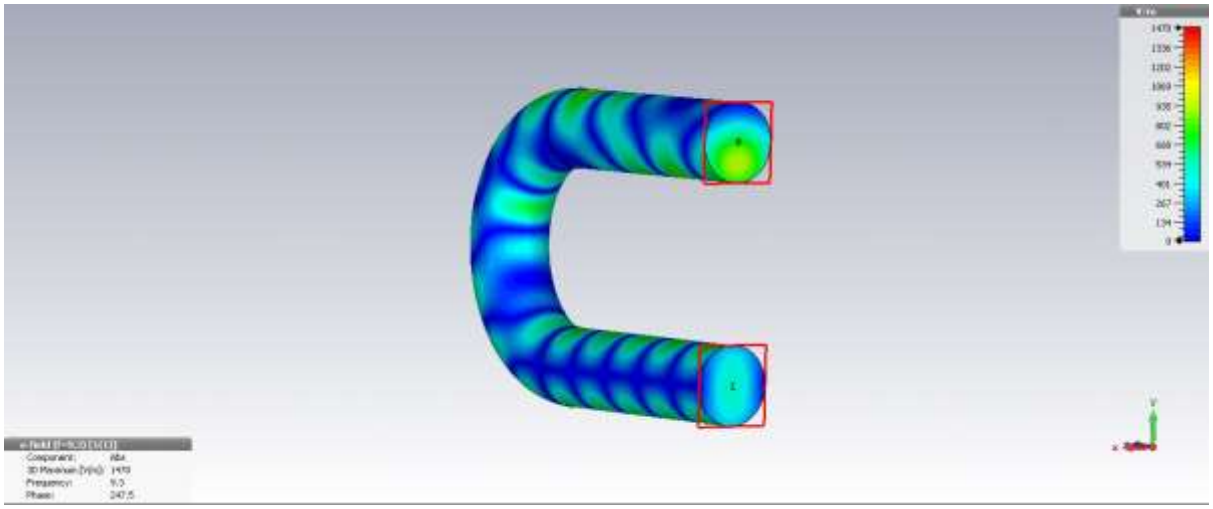

Figure 31 44.1mm radius U-bend with vertical linearly polarised signal

Figure 30 shows there is very little distortion of a signal polarised perpendicular to the bend, however there is significant mode conversion of a signal polarised parallel to the bend, figure 31. Looking at the S-parameters, figure 32, the strongest signals are S2(1),1(1) and S2(3),1(1). These signals correspond to the signal at port 2 due to the input of the $TE_{1,1}$ mode at port 1. S2(1) is the $TE_{1,1}$ mode at port 2. S2(3) is the $TM_{0,1}$ mode at port 2.

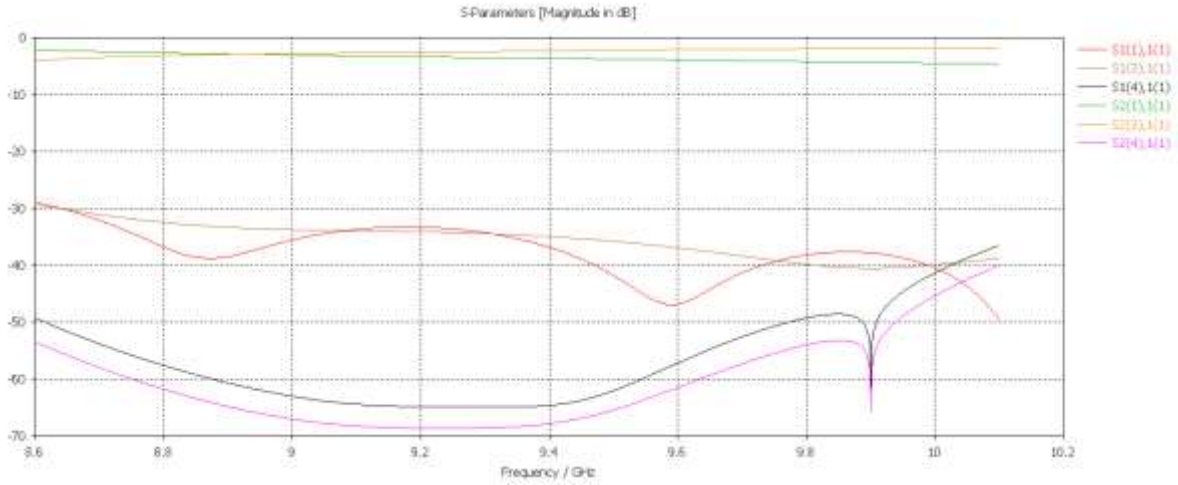

Figure 32 S-parameters for 44.1mm radius U-bend with vertical linearly polarised signal

Increasing the radius of the bend has no effect on the horizontal linearly polarised signal with little to no mode conversion. It does however have an effect on the vertical linearly polarised signal where it changes the frequency at which there is a minimum

Distribution A Distribution Approved for Public Release: Distribution Unlimited

of mode conversion. For a frequency centred on 9.3GHz a radius of 77.175mm was found to minimise the mode conversion (5.25 times radius of waveguide). The results are shown in figure 33, figure 34 and figure 35.

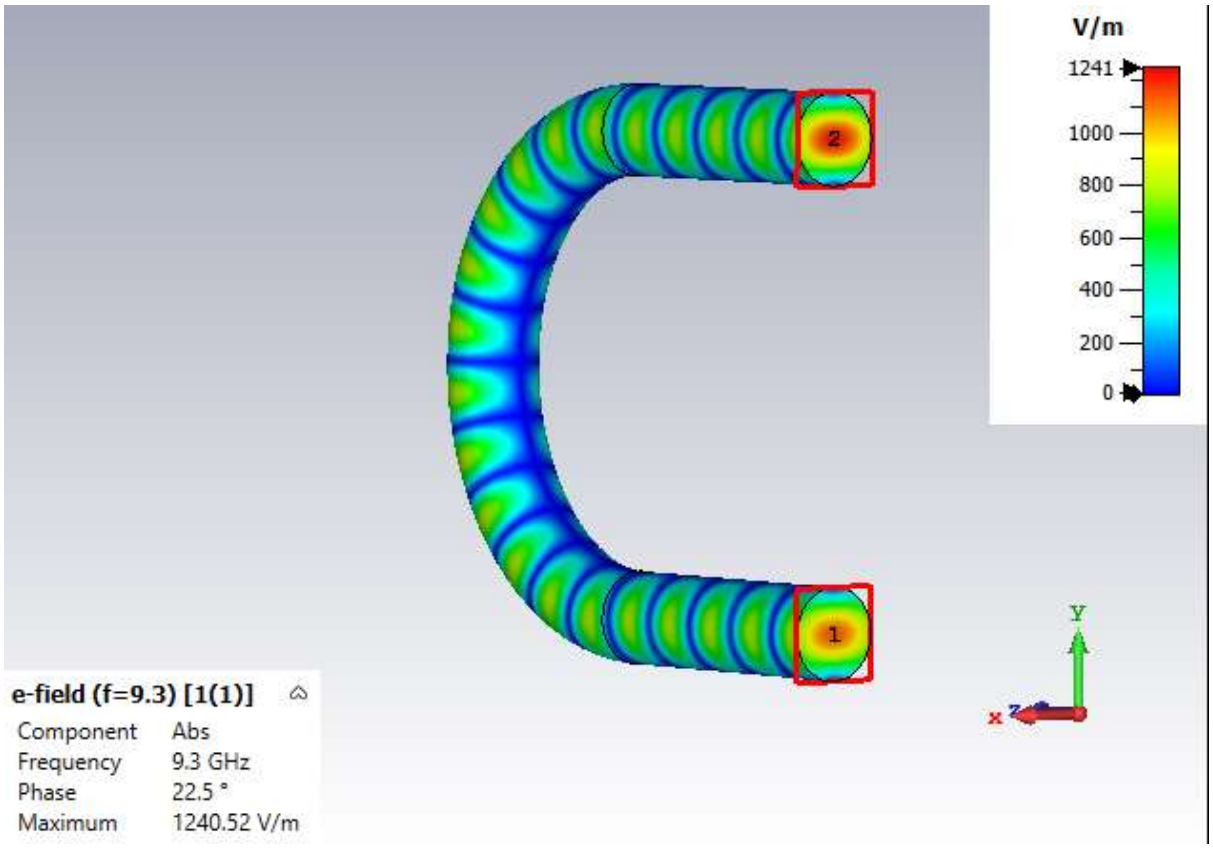

Figure 33 77.175mm radius U-bend with horizontal linearly polarised signal

Distribution A Distribution Approved for Public Release: Distribution Unlimited

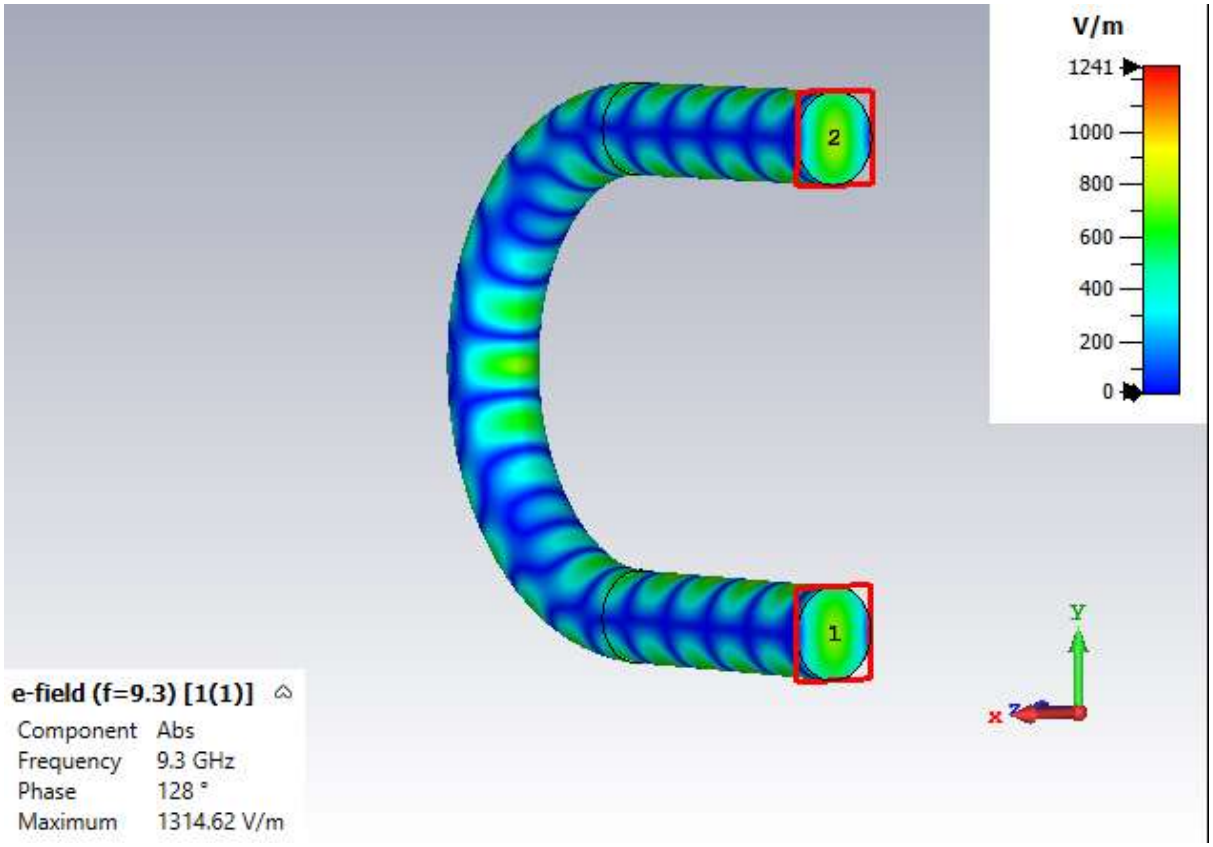

Figure 34 77.175mm radius U-bend with vertical linearly polarised signal

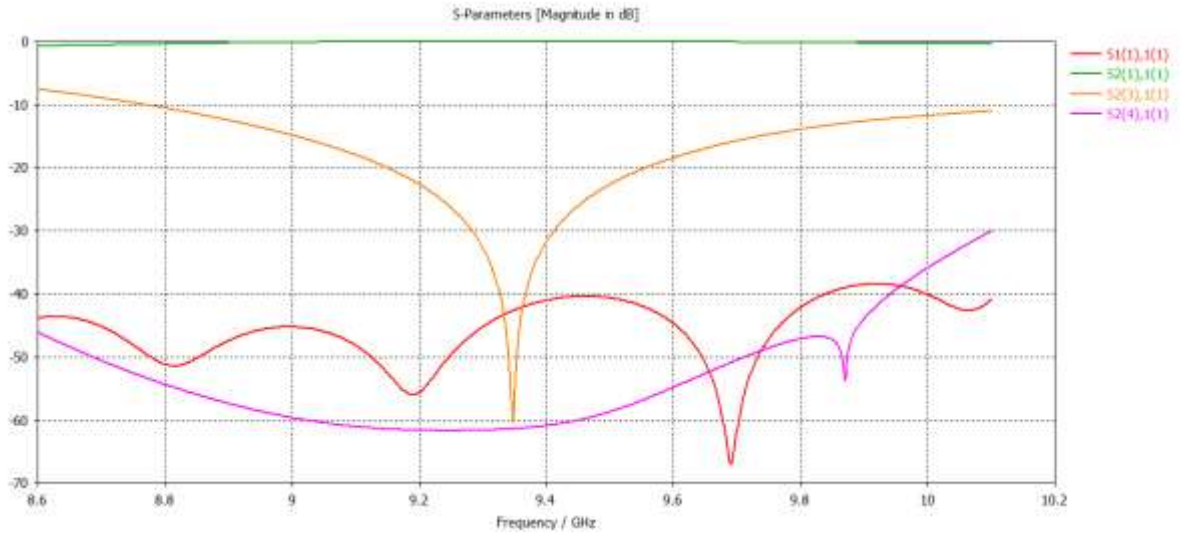

Figure 35 S-parameters for 77.175mm radius U-bend with vertical linearly polarised signal

This shows that there is an optimal radius that inhibits mode conversion. However it is important to notice that the bend does introduce a slight phase difference between the

Distribution A Distribution Approved for Public Release: Distribution Unlimited

two linear polarisations, which would need to be compensated for with a segment of phase shifting waveguide (this can be easily implemented by inserting an elliptical or corrugated waveguide segment aligned with one of these linear polarisations).

4. Potential for novel fabrication of helically corrugated pulse compressors

4.1 Conventional fabrication approaches

The helically corrugated waveguide is not trivial to fabricate. It is inherently a 3D surface, and as in some parts of the spectrum the group velocity is quite low, around one tenth the speed of light it is important that the conductivity of the walls is high. The requirement for a high performance wall material in practical terms limits the choice to copper, or copper overflashed with silver or gold. It is prohibitively expensive to manufacture in solid with such precious metals. Flashing with silver gives the highest surface conductivity possible with a metal, however it must be maintained in a very clean environment due to the rapid oxidation of silver. Coating with gold slightly reduces the electrical performance of the surface, however it brings the benefit that the relatively inert gold stabilises the copper surface which would otherwise also oxidise if more slowly than the silver flashed surface. Both techniques based on thin film coatings are of course mechanically vulnerable to scratching and damage whilst under high thermal load or during bakeout if operated under vacuum there may be a risk of delamination. Additionally shock ‘pulse’ heating of the deposited surface (which is likely to be relatively poorly thermally coupled to its substrate) could become an issue, increasing losses due to the poor thermal dissipation and limiting peak and average power handling. In general, the advantages of coating with silver are rarely worthwhile, the benefits of gold coating are likely to be more substantial, however it is probably best overall to use copper and to keep the surfaces as clean as possible.

The geometry may be created with a few primary techniques: End milling is highly effective where a milling cutter is inserted into the end of the waveguide and is used to remove material around the circumference following a computer generated path. The method does have difficulties however:

Distribution A Distribution Approved for Public Release: Distribution Unlimited

1) The corrugation depth and mean waveguide radius defines the machine tool. The tool stalk must be of finite radius r_t whilst the tools overall radius must fit inside the minimum radius of the corrugated waveguide (r_0-l) as defined in section 1. The flutes must reach at least 2l beyond the radius of the tool stalk, hence the maximum value of r_t is (r_0-3l). Considering the waveguide discussed here, with $r_0 = 14.68mm$ and a corrugation amplitude of $l = 1.4mm$ the tool stalk radius can be relatively generous ~$10mm$ although practical considerations require additional clearances that will reduce this slightly.
2) The limited tool stalk will constrain the reach of the tool forcing the fabrication of the waveguide from relatively short sections, probably limited in length to some few times the tool stalk diameter which must then be joined along their axis. The multitude of joins can be a significant weakness in the electrical continuity of the waveguide.
3) Copper, the favoured material, machines poorly. The machining techniques might be more effectively deployed on aluminium or brass material which are much more amenable in the way they cut under action of the tools. Copper tends to generate swarf that can interfere with the cutting action of the tool increasing vibration- limiting still further the reach that can be expected for a given tool and limiting the surface quality that may be achieved.

Spark erosion (Electro-Discharge Machining or EDM) with a 4-axis EDM machine tool can eliminate some of these issues with conventional machine tools. In particular this type of machining changes the reach limitation from one associated with the tool stiffness to one defined by the machine's translation range (typically rather larger). However the process is slow and causes extreme wear on the electrodes due to the high conductivity of the copper workpieces (the cutting electrodes are typically fabricated from copper and wear at a rate similar to the workpiece). The surface finish is typically not as smooth as for the other techniques mentioned here. The production of helical taper transitions poses particularly difficult problems for the EDM method.

Most of the helically corrugated waveguide components currently in use in both pulse compressors and vacuum tubes have been fabricated by a 'lost-aluminum' process where the negative of the required shape is machined in aluminum- this can be achieved without long reach on a four axis CNC mill with special 'ball-nose' like cutters

Distribution A Distribution Approved for Public Release: Distribution Unlimited

giving an excellent surface finish. The copper is electrodeposited onto the aluminium to a thickness of several mm, and the aluminium is etched by a strong alkali leaving the required copper structure. This produces vacuum compatible components, with an excellent surface finish and cleanliness with an aspect ratio primarily limited by the size of the electrodeposition bath (along with considerations of rigidity of the component).

It should be noted that all of these techniques critically demand a relatively thick wall copper structure- this defines the weight of the device. A three-fold pulse compressor such as described in this report can readily be carried by one person, a five-fold pulse compressor with similar compression ratio is significantly heavier and would be difficult for one person to handle.

4.2 CNTs: Potential alternative fabrication methods

The development of Carbon Nano-Tubes (CNTs) may prove to be a disruptive (that is to say extremely beneficial) material technology. They have, as discrete nanoscale objects, remarkable electrical and thermal transport properties whilst being mechanically exceptionally robust. Potential areas of application include acting in place of metals for strands in electrical wiring[xiii] as tips for field emitters[xiv] and as an alternative for modern composite materials used in fabrication. It has recently become possible to fabricate CNTs into films, with a high degree of alignment for the CNTs.

In particular the electrical performance of individual CNTs shows very high electrical conductivity may be achieved, and should it be possible to achieve a sufficiently high packing density whilst retaining the high current carrying capability then these materials are likely to represent an excellent alternative to conventional metals in certain applications. A particular figure of merit that has been highlighted is the specific conductivity- the conductivity divided by the density of the media.

The conductivity of assemblies of nanotubes is reported to be highly sensitive to the detail of fabrication [xiii,xv] and subsequent post processing and the stability of the highest performing assemblies described in [xiii,xv] (which have a conductivity around one tenth that of copper) is mentioned in [xv] as requiring further research.

This is a rapidly developing field, for example in[xvi] it is reported that the specific conductivity of some samples fabricated with a refined process to ensure carefully

Distribution A Distribution Approved for Public Release: Distribution Unlimited

aligned CNT fibres can be made to exceed single crystal carbon. Measurements have also been undertaken using a section of CNT material loaded into the central conductor of a microstrip line using a range of CNT media up to a frequency of 10 GHz and by irradiation by waveguide in the range 20-30 GHz and 65-120 GHz showing subtle behaviour of the materials. In particular a marked increase in the conductivity was observed with frequency (although still meaningfully less than the conductivity of copper)[xvii].

4.2.1 Constraints and areas for further investigation

The information available about the behaviour of CNT media indicates that although remarkable conductivities have been achieved these do not yet equal the performance of copper. As this is an active field of research it seems likely that this will continue to evolve and should be watched carefully over the coming years. The dispersion of the pulse compressor waveguide features regions of relatively low group velocity which are particularly sensitive to surface losses, see figure 10. The effect of using pure copper as opposed to perfect conductor was illustrated in section 3.2.3. This arises as the surface loss per unit area is $\propto {}^{1}/_{\sqrt{\sigma}}$ with σ the electrical conductivity. Clearly any material used for the compressor walls must closely approach the conductivity of copper if the input energy is not to be significantly attenuated.

It seems clear from the literature that the conductivity (both thermal and electrical) of CNTs is a strong function of the relative orientation of the energy/current flux and the fibres. Indeed much of the effort in improving performance is associated with increased alignment of the fibres. Certain types of microwave waveguide carry well-aligned currents: Examples include co-axial lines and striplines. In general however hollow waveguide modes drive currents in both axial and azimuthal directions and therefore it will not be possible to align the polarisation of the fibres to match both components of the current. The currents associated with the hybrid modes in the microwave pulse compressor are particularly complex and are hence likely to suffer increased losses due to the one-dimensional nature of the conductivity of CNT material. It would however be interesting to explore whether the anisotropy of wall conductivity could offer other functional behaviour.

Distribution A Distribution Approved for Public Release: Distribution Unlimited

The anisotropic nature of the thermal conductivity is likely also to pose a difficulty in a system operating at high average power. It may be difficult to exchange heat dissipated in the inner surface of the waveguide walls with the environment, limiting the average power handling capability.

It may be possible to take advantage of the strength and light-weight nature of the CNT material by using it to provide a strong carrier for a copper inner wall. This wall would provide an isotropic layer providing it was a few skin depths thick: At 10 GHz this requirement implies a layer of a few microns of copper. In this case the CNTs electrical performance would be irrelevant and one may use disordered material which is relatively easier to produce. It is likely that the average power handling will be less than for solid copper due to the thermal transport difficulties across the boundary layer and across the CNT support structure, however this may not always be a limiting factor for applications as discussed in section 3.2.4, whilst the weight benefits may more than compensate. This should be caveated with the following considerations: the flatness of the inner surface of the copper material must be considerably smaller than the skin depth (i.e. of order 100nm) in order to avoid a significant effective increase in the losses due to the path increase caused by the material roughness (which manifests itself as an increase in the effective resistivity). Moreover it has already been noted that CNTs with their sharp ends can be effective field emitters. It will be essential that the copper overlay ensures that no fibres with small-scale sharp features are exposed on the inside of the waveguide (whether metallic of carbon), as this will give rise to significant field enhancement and reduce the peak power handling capability.

The authors recommend the next step would be to fabricate and test a smooth wall copper-coated CNT waveguide element for comparison with a conventional section of waveguide.

5. Conclusion

A dispersive pulse compressor based on a helical corrugated waveguide operating on pulses with a frequency from 9GHz to 9.6GHz has been studied, particularly with the objective of increasing the spectral range that can be addressed by such a compressor. A number of techniques were implemented to establish the dispersion of the helically corrugated waveguide, with all methods showing good agreement,

Distribution A Distribution Approved for Public Release: Distribution Unlimited

particularly between the analytic method and direct measurement. Critically both the simulations and the experimental measurement revealed that the dispersion of the uncoupled mode (i.e. one of the two circular polarisations of the $TE_{1,1}$ mode), expected to approximate that of a smooth waveguide has no apparent stopbands where the radiation gets converted into alternative trapped modes, or regions of strongly varying group speed. The same measurements showed very strong (and expected) stopband behaviour above the knee of the dispersion for the coupled mode. This indicates that it would be possible to combine two (but no more than two) dispersive compressors with opposite chirality in a compact series chain, enhancing the spectral coverage. From the dispersion an optimum chirp input signal was calculated for the pulse compressor and computer simulations showed a compression factor of over 25 could be achieved when the walls are made of a perfect electrical conductor. Changing the walls of the waveguide to copper reduces the compression by about 15%.

Assuming a low duty cycle so that there is no risk of thermal load damaging the structure of the waveguide the maximum output power in dry air at atmospheric pressure is approximately 1.3MW for long pulses. For short pulses of a few nanoseconds data in the literature indicates this can be increased by a factor of 4 to 5.2MW. By filling the pulse compressor with an electronegative gas the peak output power can prospectively be increased still further to 48MW, and if the pulse compressor is in vacuum peak output powers of a few GWs may be possible. Yet higher powers may be realised by a 5-fold variant of the pulse compressor, however this would not be able to operate over more than a limited spectral range.

As the objective of the project was to seek ways of increasing the spectral range over which the pulse compressor can be effectively used, it was essential to address the bandwidth limitations imposed by the circular polarisers, which convert between linearly and circularly polarised radiation. A polariser with a periodic corrugation was numerically demonstrated to provide superior bandwidth to the traditional elliptically deformed waveguide method. This was verified in experimental measurement, although it should be noted that it is significantly more complicated to manufacture.

Numerical investigations were conducted of the proposed method of increasing the spectral range of the pulse compressor by using two sections of helical waveguide in series, and also a possible method of making the compressor more compact by folding

Distribution A Distribution Approved for Public Release: Distribution Unlimited

it using U-bend sections of waveguide. These methods could be potentially combined by allowing the two ‘series’ sections of the dispersive compressor to lie alongside each other. The series pulse compressor works by exploiting the sensitivity of the compressor to the direction of circular polarisation of the input radiation, by arranging the two compressors to have the opposite chirality. Thus a high frequency chirp with a given circular polarisation can be effectively compressed by the first compressor (and merely transmitted by the second compressor), whilst the lower frequency chirp with the opposite circular polarisation is compressed by the second compressor. The simulations demonstrate the effectiveness of this method.

A next step would be to fabricate the components for such a double pulse compressor and the U bends required for folding the structure for testing on network analysers and at moderate power levels (hundreds of kW peak).

Recent literature on CNT film properties has been reviewed. At present even the best CNT materials fall below the electrical properties of copper, whilst the an-isotropic conductivity is likely to affect both the loss and the modes which a waveguide can support, the potential for using the CNT materials as light-weight support structures for a metallic inner wall coating certainly merits further investigation. A logical next step would be to prepare a smooth waveguide to assess the relative performance of such a component against a component fabricated from copper in the conventional way.

6. Acknowledgements

The authors would like to thank the funders who have enabled this research. In addition to the direct support for this specific project from the AFOSR: FA9550-18-1-7014 for which this report is prepared, this research was enabled by long standing support from the UK dstl and the UK EPSRC. Helpful conversations with Prof. A.W. Cross, Dr’s. C.G. Whyte, L. Zhang, C.W. Robertson are gratefully acknowledged. Mr. D. Barclay is thanked for his engineering support.

Distribution A Distribution Approved for Public Release: Distribution Unlimited

7. References

[i] Denisov G.G., Bratman V.L., Cross A.W., He W., Phelps A.D.R., Ronald K., Samsonov S.V. and Whyte C.G., 1998, 'Gyrotron traveling wave amplifier with a helical interaction waveguide', Phys. Rev. Lett., **81**, pp5680-5683

[ii] Bratman V.L., Cross A.W., Denisov G.G., He W., Phelps A.D.R., Ronald K., Samsonov S.V., Whyte C.G. and Young A.R., 2000, 'High-gain wide-band gyro-traveling wave amplifier with a helically corrugated waveguide', Phys. Rev. Lett., **84**, pp2746-2749

[iii] Samsonov S.V., Ronald K., Denisov G.G., Young A.R., Bratman V.L., Phelps A.D.R., Cross A.W., Konoplev I.V., He W., Thomson J. and Whyte C.G., 2004, 'Dispersion of helically corrugated waveguides: analytical, numerical and experimental study', Phys. Rev. E, **70**, Art. No. 046402

[iv] Samsonov S.V., Phelps A.D.R., Bratman V.L., Burt G., Denisov G.G., Cross A.W., Ronald K., He W. and Yin H., 2004, 'Compression of frequency-modulated pulses using helically corrugated waveguides and its potential for generating multigigawatt rf radiation', Phys. Rev. Lett., **92**, art. 18301

[v] Burt G., Samsonov S.V., Phelps A.D.R., Bratman V.L., Ronald K., Denisov G.G., He W., Young A.R., Cross A.W. and Konoplev I.V., 2005, 'Microwave pulse compression using a helically corrugated waveguide', IEEE Trans. on Plasma Science, **33**, 661-667

[vi] McStravick M., Samsonov S.V., Ronald K., Mishakin S.V., He W., Denisov G.G., Whyte C.G., Bratman V.L., Cross A.W., Young A.R., MacInnes P., Robertson C.W., Phelps A.D.R., 2010, 'Experimental results on microwave pulse compression using helically corrugated waveguide', J. Appl. Phys., **108**, Art.054908

[vii] Bratman, V. L.,Denisov, G. G., Samsonov, S. V.,Cross, A. W. Ronald, K. and Phelps, A. D. R., 2007, 'Method for achievement of a multigigawatt peak power by compressing microwave pulses of a relativistic backward-wave oscillator in a helical waveguide', Radiophys, and Quantum Electronics, **50**, pp36-48

[viii] Zhang L., Mishakin S.V., He W., Samsonov S.V., McStravick M., Denisov G.G., Cross A.W., Bratman V.L., Whyte C.G., Robertson C.W., Young A.R., Ronald K., Phelps A.D.R., 2015, 'Experimental Study of Microwave Pulse Compression Using a Five-Fold Helically Corrugated Waveguide', IEEE Trans. Micro. Theory and Tech., **63,** pp1090-1096

[ix] He W., Donaldson C.R., Zhang L., Ronald K., Phelps A.D.R., Cross A.W., 2017, ' Broadband Amplification of Low-Terahertz Signals Using Axis-Encircling Electrons in a Helically Corrugated Interaction Region', Phys. Rev. Lett., **119**, art. 184801

[x] Yalandin M.I., Shpak V.G., Shunailov S.A., Oulmaskoulov M.R., Ginzburg N.S., Zotova I.V., Novozhilova Y.V., Sergeev A.S., Phelps A.D.R., Cross A.W., Wiggins S.M. and Ronald K, 2000, 'Generation of powerful subnanosecond microwave pulses in the range of 38-150 GHz', IEEE Trans. on Plasma Science, **28**, pp1615-1619

[xi] Gilmour A.S., 1986, 'Microwave Tubes', Artech House, Norwood (MA,USA)

[xii] Gunin A.V., Klimov A.I., Korovin S.D., 1998, 'Relativistic X-Band BWO with 3-GW Output Power', IEEE Trans. Plasma Sci.,**26**, 326-331

[xiii] Lekawa-Raus A., Patmore J., Kurzepa L., Bulmer J., Koziol K., 2014, 'Electrical Properties of Carbon Nanotube Based Fibres and Their Future Use in Electrical Wiring', Adv. Funct..Mater., **24**, pp3661-3682

[xiv] Fairchild S.B., Bulmer J.S., Sparkes M.,Boecki J., CahayM., Back T., Murray T., Gruen G., Lange M., Lockwood N.P., Orozco F., O'Neill W., Paukner C., Koziol K.K.K, 2014, 'Field emission from laser cut CNT fibres and films', J. Mater.Res., **29**, pp392-402

[xv] Dini Y., Faure-Vincent J., Dijon J., 2019, 'How to overcome the electrical conductivity limitation of carbon nanotube yarns drawn from carbon nanotube arrays', Carbon, **144**, pp301-313

[xvi] Bulmer J.S., Mizen, J.E., Gspann T.S., Kaniyoor A., Ryley J.B., Kiley P.J., Sparkes M.R., O'Neill B., Elliott J.A., 2019, 'Extreme stretchin of high G:D ratio carbon nanotube fibres using super-acid', Carbon, **153**, pp725-736

[xvii] Bulmer J.S., Martens J., Kurzepa L., Gizewski T., Egilmez M., Blamire M.G., Yahya N., Koziol K.K.K., 2014, 'Microwave Conductivity of Sorted CNT Assemblies', Sci. Reports, **4**, art 3762

Distribution A Distribution Approved for Public Release: Distribution Unlimited